Chebyshev-Taylor parameterization of stable/unstable manifolds for periodic orbits: implementation and applications

J.D. Mireles James
Maxime Murray
Department of mathematical sciences, Florida Atlantic University, 777 glades road
Boca Raton, Florida, 33431, United States of America
jmirelesjames@fau.edu
mmurray2016@fau.edu

This paper develops a computational method for studying stable/unstable manifolds attached to periodic orbits of differential equations. The method uses high order Chebyshev-Taylor series approximations in conjunction with the parameterization method – a general functional analytic framework for invariant manifolds. The parameterization method can follow folds in the embedding, recovers the dynamics on the manifold through a simple conjugacy, and admits a natural notion of a-posteriori error analysis. The key to the approach is the derivation of a recursive system of linear differential equations describing the Taylor coefficients of the invariant manifold. We find periodic solutions of these equations by solving a coupled collection of boundary value problems with Chebyshev spectral methods. We discuss the performance of the method for the Lorenz system, and for circular restricted three and four body problems. We also illustrate the use of the method as a tool for computing cycle-to-cycle connecting orbits.

Key words. periodic orbit, (un)stable manifold, parameterization method, boundary value problems, automatic differentiation, Chebyshev polynomials

1. Introduction

Periodic solutions of differential equations are the basic building blocks of complicated dynamical phenomena. A first step toward understanding the global dynamics of a nonlinear system is to study periodic orbits as well as any connecting orbits between them. Since a heteroclinic/homoclinic orbit will approach a periodic solution along its local stable/unstable manifolds, computational methods for studying these manifolds are of great interest. See any of the works [Canalias and Masdemont, 2006; Font et al., 2009; Jorba, 1999; Jorba and Masdemont, 1999; Jorba and Villanueva, 1998; Krauskopf et al., 2005; Masdemont, 2011; Osinga, 2003; Simó, 1998, 1988, 1989] for more discussion, but be warned that this list hardly scratches the surface of the relevant literature. A schematic description of the stable manifold of a periodic orbit, along with an actual stable manifold in the Lorenz system are illustrated in Figure 1.

The stable/unstable normal bundles of a periodic solution approximate the stable/unstable manifolds to first order, and these bundles are obtained by studying the equations of first variation – or equivalently – by solving certain periodic eigenvalue problems. Higher order jets of the invariant manifold could be studied via higher order equations of variation, however the complexity of these equations grows exponentially with the order. More efficient methods for studying the jets reformulate the invariant manifold as the solution of an operator equation, and study the operator equation via semi-numerical methods.

The parameterization method is a general functional analytic framework for studying invariant manifolds [Cabré et al., 2003a,b, 2005; Canadell and Haro, 2014; Figueras and Haro, 2012, 2013; Haro and de la

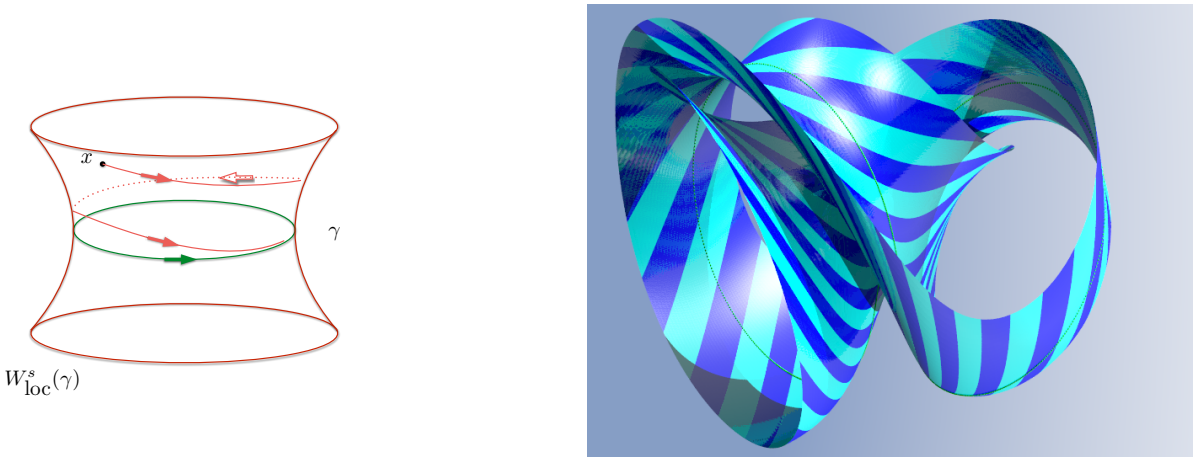

Fig. 1. The local stable manifold attached to a periodic orbit $\gamma(t)$: (LEFT) schematic representation of the stable manifold, i.e. it is the union of all solutions accumulating at γ as $t \to \infty$ (periodic orbit shown here as the green loop). The unstable manifold is the same but with orbits approaching the periodic orbit asymptotically in backward time. (RIGHT) local stable manifold of an actual periodic orbit near the Lorenz attractor. This manifold is computed using the techniques of the present work. In particular, changes in color in the figure indicate the transitions from one Chebyshev domain to another.

Llave, 2006a,b, 2007] whose goal is to find a chart/covering map conjugating the dynamics on the invariant manifold to a simple and well understood model. We view the conjugacy as an operator equation for the unknown chart, so that the problem is then susceptible to any appropriate numerical method for solving the operator equation.

We refer to the operator equation as the *invariance equation* for the parameterization method. In the case of stable/unstable manifolds attached to equilibrium and periodic solutions, the parameterization is not required to be a graph hence is able to follow folds in the embedding. See again Figure 1. Since the invariance equation is based on a conjugacy, the method provides the dynamics on the manifold in addition to the embedding. By now there is a small industry devoted to the parameterization method, and a review of the literature would take us far afield. Instead we refer the interested reader to the recent book on the subject [Haro et al., 2016], where many examples and much discussion of the literature is found.

The present work is not the first numerical treatment of parameterized stable/unstable manifolds for periodic orbits, and indeed we build on the earlier studies of [Cabré et al., 2005; Castelli et al., 2015; Guillamon and Huguet, 2009; Huguet and de la Llave, 2013]. As in these earlier studies, we make a formal Taylor series arguments which reduces the invariance equation analytically prior any numerical computation. Since the coefficients of the Taylor series are themselves periodic functions, the formal power matching scheme leads to so called *homological equations* describing the unknown coefficients. In the present case of a periodic orbit, the homological equations are linear ordinary differential equations with periodic coefficients and periodic forcing. It is these homological equations which we solve recursively using numerical methods, leading to a high order approximation of the stable/unstable manifold which is accurate far from the periodic orbit.

In the earlier works just cited the differential equations – describing the periodic orbit, describing the normal bundles, and the homological equations describing the higher order jets – are all solved using Fourier spectral methods. Fourier methods are both efficient and accurate when applied to periodic solutions of moderate length. This efficiency is due in part to the fact differentiation is a diagonal operation in the transform domain, and in part to the fact that the FFT speeds up evaluation of nonlinearities. However, the decay rate of the Fourier coefficients gets increasingly slow as the period/harmonic complexity of the orbit grow. In practice this means that it is necessary to compute more and more Fourier coefficients, and for long enough orbits the Fourier approximation becomes impractical.

There is much recent interest in numerical methods based on Chebyshev spectral approximation of solutions to boundary value problems. A thorough review of this literature is again beyond the scope of the present work, and we refer the interested reader to [Driscoll et al., 2008; Platte and Trefethen, 2010;

Trefethen, 2007, 2013] and the references discussed there in. We are interested in the work by a number of authors which uses Chebyshev spectral methods to compute long periodic solutions of differential equations [Gameiro et al., 2016; Lessard and Reinhardt, 2014; van den Berg and Sheombarsing, 2016]. The merit of this approach is that Chebyshev spectral methods have many of the advantages of Fourier series – for example differentiation is a tri-diagonal operation in the transform domain and the fast cosine transform is available for evaluating nonlinearities – but Chebyshev series apply to non-periodic boundary value problems. Treating a periodic solution as a series of coupled boundary value problems – on smaller domains – reigns back in the decay rates of the coefficients.

Motivated by these developments, the present work applies Chebyshev methods not only the periodic orbit – but also to the computation of the normal bundles and the homological equations for the higher order jets. The result is a computational method for finding Chebyshev-Taylor expansions of the local stable/unstable manifolds attached to periodic orbits. Our method applies to more complicated orbits and their attached invariant manifolds than could be studied using only the Fourier-Taylor approach.

Remark 1.1 [Connecting orbits and extensions of local stable/unstable manifolds]. Of course computing local stable/unstable manifolds attached to periodic orbits is only a means to an end. In applications we are often interested in either using the local manifolds to compute connecting orbits, or to grow larger portions of the invariant manifold in order to study the global dynamics. While in the present work we do consider a number of example computations for connecting orbits, we do not make any serious attempt to numerically grow larger local manifolds. This is because the literature on computational methods for growing invariant manifolds is extensive and well developed. The interested reader will want to consult the review paper [Krauskopf et al., 2005] for a thorough overview of the literature, and will find other powerful methods and fuller discussion in [England et al., 2005; Osinga, 2000, 2003]. We only note that the methods developed in the present work could be combined with existing continuation methods for even better results. This is especially true for methods which exploit the curvature or other differential geometric properties of the manifold.

Remark 1.2 [Automatic differentiation and polynomial nonlinearities]. Multiplying and taking powers of Taylor and Chebyshev series is a relatively straight forward endeavor, using the Cauchy product formula/discrete cosine convolution formula respectively. Then semi-numerical methods for polynomial nonlinearities are especially transparent in these bases.

In the present work we are interested in applications coming from celestial mechanics which involve non-polynomial terms. We exploit so called methods of *automatic differentiation* to reduce to polynomial problems, albeit in a higher dimensional phase space. This is discussed in detail for Fourier series in [Lessard et al., 2015], but the idea is to append additional polynomial differential equations whose solutions correspond to the transcendental nonlinearities of the original problem.

The use of automatic differentiation is a convenience rather than a necessity, as FFT algorithms can be used for both Taylor and Chebyshev series multiplication. These algorithms could be used to evaluate general nonlinearities. In fact, even after automatic differentiation we use the fast cosine transform to evaluate higher order polynomial nonlinearities. We prefer to use automatic differentiation schemes in the present work as it simplifies the implementation details of our algorithms – all our computations are reduced to Newton's method for large polynomial systems. It also simplifies a-posteriori error analysis for the method, which when followed to its logical conclusion provides mathematically rigorous validated error bounds for the parameterizations. Using the parameterized manifolds computed here as ingredients in computer assisted proofs is the topic of upcoming work by the authors.

2. Review of the parameterization method

As already mentioned in the introduction, the parameterization method is much more general than what we actually use in the present work. We refer the reader again to the book [Haro et al., 2016]. In the following section we review some basic notions in the very simple setting of an orientable local manifold associated with one stable/unstable Floquet exponent. Generalities such as multiple stable/unstable exponents, complex conjugate exponents, and non-orientable bundles are discussed in detail in [Castelli et al.,

2015]. The methods of the present work apply in these more general setting with only obvious modifications. We focus on the one dimensional case to simplify the exposition. That being said, parameterization of stable/unstable manifolds for periodic orbits of non-polynomial vector fields has not been appeared in the literature, and so in the sequel we discuss the automatic differentiation in some detail.

2.1. *Parameterization of the stable/unstable manifold attached to a periodic orbit*

Let $\Omega \subset \mathbb{R}^M$ be an open set and $g\colon \Omega \to \mathbb{R}^M$ be a real analytic vector field. Suppose that $\gamma\colon \mathbb{R} \to \mathbb{R}^M$ is a T-periodic solution of the first order ordinary differential equation

$$\dot{x} = g(x),$$

that is we assume that $\gamma'(t) = g(\gamma(t))$ with $\gamma(t+T) = \gamma(t)$ for all $t \in \mathbb{R}$. Suppose also that γ has one stable Floquet exponent

$$\lambda \in \mathbb{R}, \qquad \text{with} \qquad \lambda < 0,$$

so that (by the stable manifold theorem) there exists a two dimensional manifold of solutions which converge exponentially fast to the periodic orbit γ. Let $v\colon \mathbb{R} \to \mathbb{R}^M$ denote the stable normal bundle of $\gamma(t)$, associated with the exponent λ. We assume that v is an orientable bundle, so that $v(t)$ is T periodic as well. We note that (v, λ) solve the eigenvalue problem

$$\frac{d}{dt}v(t) = Dg(\gamma(t))v(t) - \lambda v(t),$$

subject to some normalization, perhaps $\|v(t)\| = 1$ for all $t \in \mathbb{R}$ (though in numerical applications we will choose other normalizations).

The goal of the parameterization method is to find a smooth function $P\colon [0,T] \times [-1,1] \to \mathbb{R}^M$ solving the invariance equation

$$\frac{\partial}{\partial t}P(t,\sigma) + \lambda\sigma\frac{\partial}{\partial \sigma}P(t,\sigma) = g(P(t,\sigma)), \tag{1}$$

subject to the first order constraints

$$P(t,0) = \gamma(t), \tag{2}$$

and

$$\frac{\partial}{\partial \sigma}P(t,0) = v(t). \tag{3}$$

Then geometric content of Equation (1) is illustrated in Figure 2, but one easily checks that the image of P is a stable manifold.

To see this let P be a smooth solution of Equation (1) subject to the first order constraints. Choose any $\sigma_0 \in (-1,1)$ and define the curve $x\colon [0,\infty) \to \mathbb{R}^M$ by

$$x(t) = P(t, e^{\lambda t}\sigma_0).$$

Then

$$\begin{aligned}
\frac{d}{dt}x(t) &= DP(t, e^{\lambda t}\sigma_0)\begin{pmatrix} 1 \\ e^{\lambda t}\lambda\sigma_0 \end{pmatrix} \\
&= \frac{\partial}{\partial t}P(t, e^{\lambda t}\sigma_0) + \lambda\sigma_0 e^{\lambda t}\frac{\partial}{\partial \sigma}P(t, e^{\lambda t}\sigma_0) \\
&= g(P(t, e^{\lambda t}\sigma_0)) \\
&= g(x(t)),
\end{aligned}$$

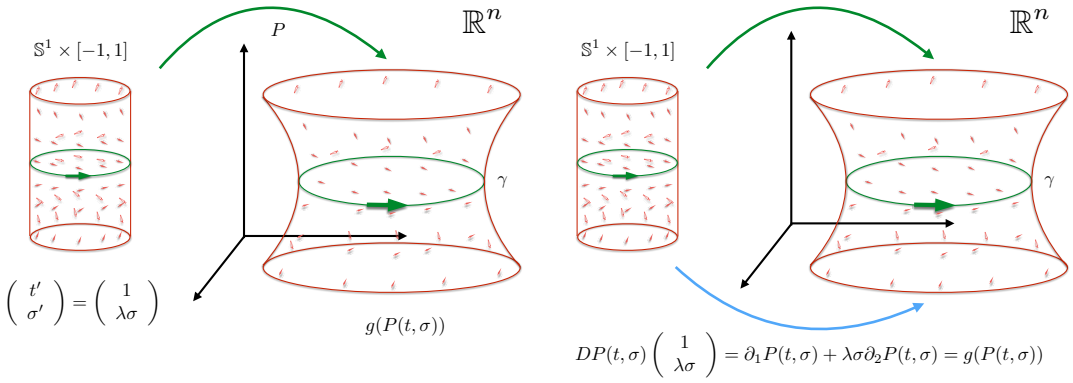

Fig. 2. Geometric meaning of Equation (1): (LEFT) the model space for the stable manifold is the cylinder $\mathbb{S}^1 \times [-1,1]$, which we endow with the model vector field $t' = 1$, $\sigma' = \lambda\sigma$. Here λ is the stable Floquet exponent of the periodic orbit $\gamma(t)$. Now if P is *any* mapping from the cylinder into $\mathbb{R}^M$, then g induces a vector field on the image of P by restriction. (RIGHT) The derivative of P pushes forward vector fields defined on the cylinder. The goal of the parameterization method is to find a mapping P so that the push forward of the model dynamics is equal on the image of P to the vector field induced by g. If these vector fields are equal then they have the same dynamics. But the dynamics on the cylinder are completely understood. See Figure 3.

as $e^{\lambda t}\sigma_0 \in (-1,1)$ for all $t \geq 0$. Then $x(t)$ is a solution curve for the differential equation having $x(0) = P(0,\sigma_0)$. Moreover for any $t_0 \in [0,L]$, since P is continuous we have that

$$\begin{aligned} \lim_{t\to\infty} x(t) &= \lim_{t\to\infty} P(t_0, e^{\lambda t}\sigma_0) \\ &= P\left(t_0, \lim_{t\to\infty} e^{\lambda t}\sigma_0\right) \\ &= P(t_0, 0) \\ &= \gamma(t_0), \end{aligned}$$

that is, a point on the image of P accumulates at the periodic orbit γ with asymptotic phase $\gamma(t_0)$. In particular, the image of P is a local stable manifold for γ.

One can actually prove more. In particular, if P solves Equation (1) subject to the first order constraints, then P actually satisfies the flow conjugacy

$$P(s+t, e^{\lambda t}\sigma) = \Phi(P(s,\sigma), t) \tag{4}$$

for all $t \geq 0$. Here Φ is the flow generated by the vector field g. The meaning of this flow conjugacy is illustrated in Figure 3. The proof of the flow conjugacy is given for example in [Castelli et al., 2015]. In the same reference that solutions of Equation (1) are unique up to the choice of the eigenfunction $v(t)$. (Any constant multiple of v is a parameterization of the stable normal bundle, but up to this choice of scaling the solution is unique). If the solution P exists, it is as regular as g. In this case P is real analytic if g is [Cabré et al., 2003b, 2005]. Moreover, in the case of one stable exponent, there exists a choice of scaling small enough that the solution P exists, and is analytic. See [Cabré et al., 2003a, 2005; Huguet and de la Llave, 2013].

2.2. *Formal series and the reduction to homological equations*

Since P exists and is analytic it makes sense to seek a power series solution

$$P(t,\sigma) = \sum_{\alpha=0}^{\infty} A_\alpha(t)\sigma^\alpha, \tag{5}$$

where $\sigma \in (-1,1)$ and the functions $A_\alpha \colon \mathbb{R} \to \mathbb{R}^M$ are analytic and T-periodic. Plugging the power series into Equation (1), expanding the nonlinearities, and matching like powers leads to equations for the unknown Taylor coefficient functions.

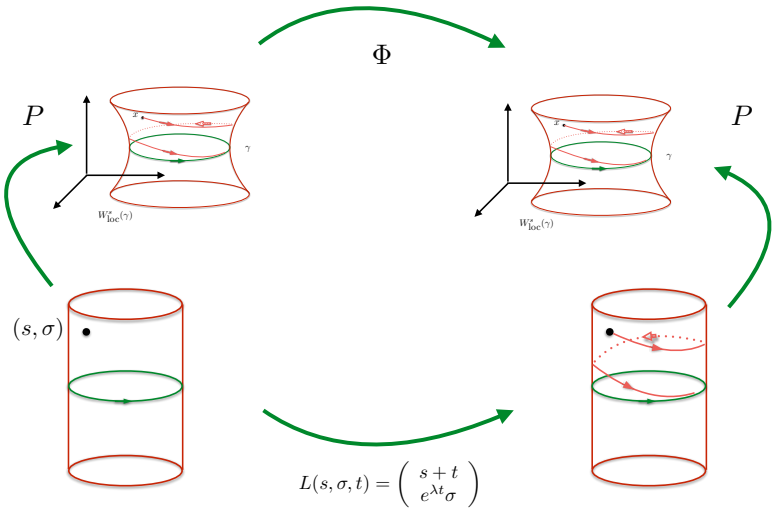

Fig. 3. Flow conjugacy generated by Equation (1): Suppose that P solves the invariance equation (1). Then the push forward of the model dynamics match the vector field induced on the image of P by g, hence the map P takes orbits on the cylinder to orbits on the image of P, i.e. P conjugates the flow on the cylinder to the flow generated by g and the above diagram commutes. Since the flow on the cylinder is known, we obtain the conjugacy given in Equation (4). In particular, since P maps the zero section in the cylinder to γ, and since all orbits in the cylinder accumulate to the zero section, the image of P is a local stable manifold for γ.

Example: the Lorenz system consider the specific case of the Lorenz field we have that $M = 3$, and the vector field g is given by

$$g(x,y,z) = \begin{pmatrix} \sigma(y-x) \\ x\rho - xz - y \\ xy - \beta z \end{pmatrix},$$

where β, ρ, σ are positive constants. Suppose that $\gamma(t) = (x(t), y(t), z(t))$ is an analytic period- T orbit with stable (or unstable) exponent λ and that $v(t) = (v_1(t), v_2(t), v_3(t))$ is an analytic T-periodic parameterization of the stable normal bundle. We look for

$$P(t,s) = \sum_{\alpha=0}^{\infty} A_\alpha(t) s^\alpha = \sum_{\alpha=0}^{\infty} \begin{pmatrix} a^{(1,\alpha)}(t) \\ a^{(2,\alpha)}(t) \\ a^{(3,\alpha)}(t) \end{pmatrix} s^\alpha$$

Then

$$A_0(t) = \gamma(t), \qquad \text{and} \qquad A_1(t) = v(t).$$

Since

$$\frac{\partial}{\partial t} P(t,s) + \lambda s \frac{\partial}{\partial s} P(t,s) = \sum_{\alpha=0}^{\infty} \left(\frac{d}{dt} A_\alpha(t) + \alpha\lambda A_\alpha(t) \right) s^\alpha,$$

and

$$g(P(t,s)) = \sum_{\alpha=0}^{\infty} \begin{pmatrix} \sigma\left(a^{(2,\alpha)} - a^{(1,\alpha)}\right) \\ \rho a^{(1,\alpha)} - a^{(2,\alpha)} - \sum_{\beta=0}^{\alpha} a^{(1,\alpha-\beta)} a^{(3,\beta)} \\ -\beta a^{(3,\alpha)} + \sum_{\beta=0}^{\alpha} a^{(1,\alpha-\beta)} a^{(2,\beta)} \end{pmatrix} s^\alpha$$

Equating and matching like powers of s leads to

$$\begin{aligned}\frac{d}{dt}A_\alpha(t)+\alpha\lambda A_\alpha(t) &= \begin{pmatrix} \sigma\left(a^{(2,\alpha)}-a^{(1,\alpha)}\right) \\ \rho a^{(1,\alpha)}-a^{(2,\alpha)}-\sum_{\beta=0}^{\alpha}a^{(1,\alpha-\beta)}a^{(3,\beta)} \\ -\beta a^{(3,\alpha)}+\sum_{\beta=0}^{\alpha}a^{(1,\alpha-\beta)}a^{(2,\beta)}\end{pmatrix} \\ &= \begin{pmatrix} \sigma\left(a^{(2,\alpha)}-a^{(1,\alpha)}\right) \\ \rho a^{(1,\alpha)}-a^{(2,\alpha)}-a^{(1,\alpha)}a^{(3,0)}-a^{(3,\alpha)}a^{(1,0)} \\ -\beta a^{(3,\alpha)}+a^{(1,\alpha)}a^{(2,0)}+a^{(2,\alpha)}a^{(1,0)}\end{pmatrix} + \begin{pmatrix} 0 \\ \sum_{\beta=1}^{\alpha-1}a^{(1,\alpha-\beta)}a^{(3,\beta)} \\ \sum_{\beta=1}^{\alpha-1}a^{(1,\alpha-\beta)}a^{(2,\beta)}\end{pmatrix}.\end{aligned}$$

Noting that

$$\begin{aligned}\begin{pmatrix} \sigma\left(a^{(2,\alpha)}-a^{(1,\alpha)}\right) \\ \rho a^{(1,\alpha)}-a^{(2,\alpha)}-a^{(1,\alpha)}a^{(3,0)}-a^{(3,\alpha)}a^{(1,0)} \\ -\beta a^{(3,\alpha)}+a^{(1,\alpha)}a^{(2,0)}+a^{(2,\alpha)}a^{(1,0)}\end{pmatrix} &= \begin{bmatrix} -\sigma & \sigma & 0 \\ \rho-z(t) & 1 & -x(t) \\ y(t) & x(t) & -\beta\end{bmatrix} A_\alpha(t) \\ &= Dg(\gamma(t))A_\alpha(t).\end{aligned}$$

Defining the functions g_α by

$$g_\alpha(A_1(t),\ldots,A_{\alpha-1}(t)) := \begin{pmatrix} 0 \\ \sum_{\beta=1}^{\alpha-1}a^{(1,\alpha-\beta)}(t)a^{(3,\beta)}(t) \\ \sum_{\beta=1}^{\alpha-1}a^{(1,\alpha-\beta)}(t)a^{(2,\beta)}(t)\end{pmatrix}.$$

We write $g_\alpha(P)$ for short. Now we seek $A_\alpha(t)$ the T-periodic solution of the equation

$$\frac{d}{dt}A_\alpha(t)-\left(Dg(\gamma(t))-\lambda\alpha\mathrm{Id}\right)A_\alpha(t)=g_\alpha(P), \tag{6}$$

which we refer to as the homological equation for P. Note that this is a linear inhomogeneous first order ordinary differential equation with periodic coefficients, and that the right hand side is independent of A_α. Indeed, g_α depends only on lower order terms. The Floquet theory guarantees that our homological equation has a unique periodic solution for each $\alpha \geq 2$. Then we recursively solve the equations to order N and have the approximate solution

$$P^N(t,s)=\sum_{\alpha=0}^{N}A_\alpha(t)s^\alpha.$$

Remark 2.1 [A-posteriori error analysis]. Truncation error analysis is treated carefully in [Castelli et al., 2017]. We also note that the analysis in this reference is independent of the basis used to represent $A_\alpha(t)$, only the implementation exploits that these functions are given as analytic Fourier series. Then the methods of this work apply directly to the expansions used in the present work. The key to the analysis in [Castelli et al., 2017] is that the approximation P^N have small defect. In the present work we only check this condition numerically, and we postpone to an upcoming work more careful analysis of the errors for our Chebyshev-Taylor approximations.

The calculations above generalizes to any polynomial vector field in the obvious way, and we have that the A_α satisfy homological equations of exactly the form given in Equation (6). Only the term $Dg(\gamma(t))$ and the form of the recursive functions $g_\alpha(P)$ depend explicitly on the form of the vector field g. In the other examples in the present work we simply write down the correct homological equations and leave the derivations as an exercise for the interested reader.

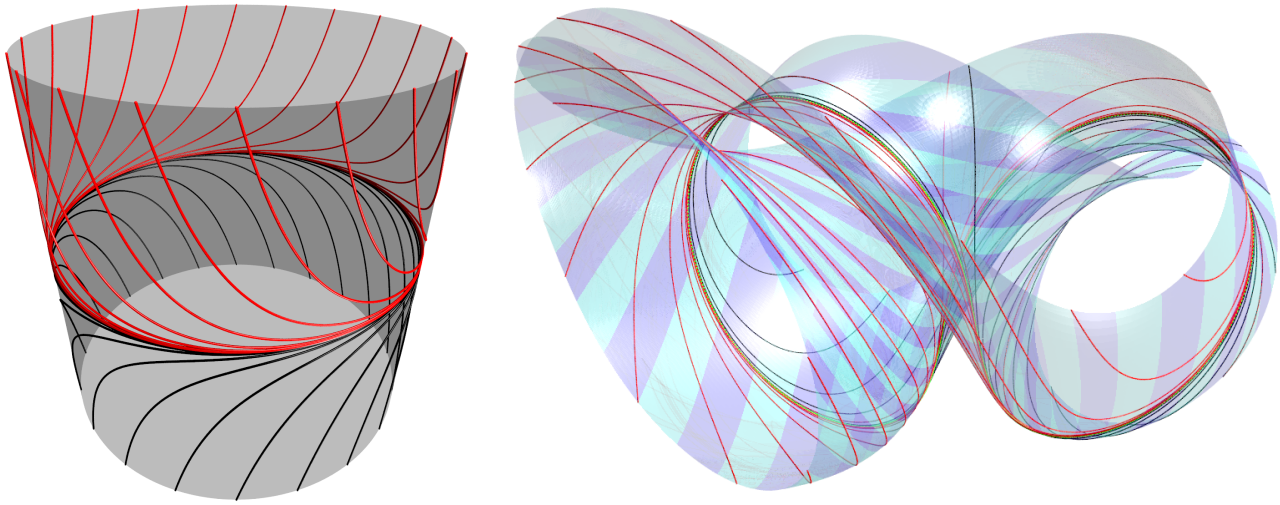

Fig. 4. The Periodic orbit AB of the Lorenz system with classical parameters in green and a Parametrized local stable manifold. Each color switch represent a different subdomain for Chebyshev. We also illustrate the conjugacy describing the dynamics on the manifold. To do this we choose a number of orbits near the boundary of the cylinder and apply the toy Flow. When these orbits are mapped by P up to the phase space, we see the more complicated and nonuniform embedding of the orbits.

3. Chebyshev Expansion for Periodic Solutions of $\dot{u}(t) = h(u(t), t)$

Since all the problems we want to solve have a similar form it makes sense to make a general study. That is the periodic orbit γ, its stable/unstable normal bundle $v(t)$, and the higher order Taylor coefficients $A_\alpha(t)$ for $2 \leq \alpha \leq N$ are all periodic solutions of non-autonomous differential equations of the form

$$\dot{u}(t) = h(u(t), t),$$

with period τ, and where $h : \mathbb{R}^M \times \mathbb{R} \to \mathbb{R}^M$. In each case we look for a solutions $v : [0, \tau] \to \mathbb{R}^M$ satisfying the boundary value problem

$$\begin{cases} \dot{v}(t) = h(v(t), t), \\ v(0) = v(\tau). \end{cases} \tag{7}$$

We develop a Chebyshev scheme to solve this class of problems.

To begin, break the solution into sub-pieces using the following mesh. Let $0 = t_0 < t_1 < t_2 < \ldots < t_D = \tau$, and for $i = 1, \ldots, D$ define $v^i(t)$ on $[t_{i-1}, t_i]$ such that

$$v^i(t) = v(t).$$

Thus, each $v^i(t)$ is a solution of $\dot{u}(t) = h(u(t), t)$. Moreover, at each of the points t_i, $1 \leq i \leq D-1$, two different pieces are defined and they must agree. Then we impose the boundary conditions

$$\begin{cases} \dot{v}^i(t) = h(v^i(t), t), \\ v^i(t_{i-1}) = v^{i-1}(t_{i-1}), \end{cases} \tag{8}$$

for $i \neq 1$, and to impose periodicity

$$\begin{cases} \dot{v}^1(t) = h(v^1(t), t), \\ v^1(t_0) = v^D(t_D). \end{cases}$$

We want to expand each piece $v^i(t)$ using Chebyshev polynomials. To do so, we first rescale the problem to the interval $[-1, 1]$. First, note that since there are no time dependence in g (the original system for

which we compute the periodic orbit) we can translate the time domain to some interval $[-L_i, L_i]$ and then rescale time $t \mapsto \frac{t}{L_i}$, so that the solution satisfies

$$\dot{v}^i(t) = L_i h(v^i(t), t), \tag{9}$$

for all $i = 1, \ldots, D$.

For the time varying case, i.e. the case of the bundles and the homological equations, the solution will depend on the lower power α of the coefficient in question. Since the bundles and Taylor coefficients of the parameterization are all periodic with *the same period*, we choose a fixed mesh for all the problems. That is, the number of subdomains D will be the same at every step. Moreover each L_i is a fixed proportion of the global period. So $L_i = p_i L$ for $p_i \in (0, 1]$ some given constant. For application unless specified we use a uniform mesh, so that $p_i = \frac{1}{D}$ for all i.

We introduce a Chebyshev expansion for each sub-piece v^i that are now defined on $[-1, 1]$. Let $v^{(i,j)} : [-1, 1] \to \mathbb{R}$ denote the $j-$th component of v^i for all $i = 1, \ldots, M$. For any $i = 1, \ldots, D$ and $j = 1, \ldots, M$, we set

$$v^{(i,j)}(t) \overset{\text{def}}{=} a_0^{(i,j)} + 2\sum_{k=1}^{\infty} a_k^{(i,j)} T_k(t), \tag{10}$$

where T_k is the $k-$th Chebyshev polynomial, which are defined as follows.

Definition 3.1. The Chebyshev polynomials $T_k : [-1, 1] \to \mathbb{R}$, $k = 0, 1, 2, \ldots$ are defined by $T_0(t) = 1$ and $T_1(t) = t$ and the recurrence relation

$$T_{k+1}(t) = 2tT_k(t) - T_{k-1}(t), \quad k \geq 1.$$

It is well known that these polynomials satisfy $T_k(\cos\theta) = \cos(k\theta)$, a fact which can be used to prove further results relating the Chebyshev series to results from Fourier analysis.

Definition 3.2. We denote the set of unknown Chebyshev coefficients of the full periodic orbit v by

$$A = \left(A^{(1)}, A^{(2)}, \ldots, A^{(D)}\right).$$

So that for every $i = 1, 2 \ldots, M$, $A^{(i)}$ represent the set of coefficients of the $i-$th piece of v defined on the interval $[t_{i-1}, t_i]$. Moreover, for a fixed k, $A_k^{(i)} \in \mathbb{R}^M$ since each has an image included in $\mathbb{R}^M$, which are all expanded using distinct Chebyshev expansions. Finally, $a_k^{(i,j)}$ denotes the $k-$th coefficient of the $j-$th dimension of v^i.

To rewrite the system as an operator defined on the set A we integrate (9) from -1 to t and obtain

$$v^i(t) - v^i(-1) = L_i \int_{-1}^{t} h(v^i(s), s)ds. \tag{11}$$

Note that $h : [-1, 1] \to \mathbb{R}^M$, since it depends on the lower and current term of the expansion of the parameterization which all are defined on $[-1, 1]$ after rescaling time. Thus it can also be expanded using Chebyshev polynomials. We set

$$h^j(v^i(t), t) = c_0^{(i,j)} + 2\sum_{k=1}^{\infty} c_k^{(i,j)} T_k(t),$$

and substitute both Chebyshev expansions in (11) to get an equation whose only time dependence is in the Chebyshev polynomials themselves/the integral. We use the recurrence formulas for the integral of the Chebyshev polynomials and rewrite the initial condition so that after simplification the Chebyshev coefficients need to satisfy a set of conditions defined in the space of Chebyshev coefficients. That is, for all $i = 1, \ldots, D$, $j = 1, \ldots, M$ and $k \geq 0$, we define

$$f_k^{(i,j)}(L, A) = 0.$$

Each $f_k^{(i,j)}(L,A)$ is given by

$$f_k^{(i,j)}(L,A) \stackrel{\text{def}}{=} \begin{cases} \left(a_0^{(i-1,j)} + 2\sum_{l=1}^{\infty} a_l^{(i-1,j)}\right) - \left(a_0^{(i,j)} + 2\sum_{l=1}^{\infty} a_l^{(i,j)}(-1)^l\right), & \text{if } k = 0 \\ 2ka_k^{(i,j)} + L_i c_{k\pm1}^{(i,j)}, & \text{if } k > 0. \end{cases} \tag{12}$$

Definition 3.3. We write $c_{k\pm1}$ to denote $c_{k\pm1} := c_{k+1} - c_{k-1}$.

We omit the derivation of the operators $f_k^{(i,j)}$. For further details, and to see why the term $k = 0$ does not depend on the vector field but only on the boundary condition, we refer to [Lessard and Reinhardt, 2014].

The boundary condition provides the initial component for the new problem, that is for the case $f_0^{(i,j)}$. So we use the form given in Equation (12) for every subintervals except for the case $i = 1$, for which we use

$$f_0^{(1,j)}(L,A) = \left(a_0^{(D,j)} + 2\sum_{l=1}^{\infty} a_l^{(D,j)}\right) - \left(a_0^{(1,j)} + 2\sum_{l=1}^{\infty} a_l^{(1,j)}(-1)^l\right). \tag{13}$$

The operator involves coefficients of the Chebyshev expansion of h, but we need to write in terms of the unknowns A. To do so, note that the Chebyshev expansion of a sum (or difference) of two functions f and g will be given by the sum (or difference) of the Chebyshev coefficients of f and g. Since we assume h to be polynomial, the only other case to handle is a product, to get back to the coefficients of the original function we use the following Lemma.

Lemma 1. *If $f(t)$ and $g(t)$ are expanded with Chebyshev series so that*

$$f(t) = a_0 + 2\sum_{k=1}^{\infty} a_k T_k(t) \quad \textit{and} \quad g(t) = b_0 + 2\sum_{k=1}^{\infty} b_k T_k(t),$$

then $f(t)g(t) = (a*b)_0 + 2\sum_{k=1}^{\infty}(a*b)_k T_k(t)$. Here $*$ denotes the discrete convolution product

$$(a*b)_k = \sum_{\substack{k_1+k_2=k \\ k_1,k_2\in\mathbb{Z}}} a_{|k_1|} b_{|k_2|}.$$

Therefore, we can completely rewrite each $f_k^{(i,j)}$ without the coefficients c_k. To compute an approximation of the solution, we consider a finite dimension approximation of the operator

$$F = \left\{ f_k^{(i,j)} : 1 \le i \le D, 1 \le j \le M, 0 \le k \le m-1 \right\},$$

so that $F : \mathbb{R}^{mMD} \to \mathbb{R}^{mMD}$. Note that the boundary value conditions introduce a dependence between each subdomain. Therefore we need to solve for every pieces at the same time. In the case $\alpha \ge 2$ one can directly use Newton's method to find $\bar{A}$ such that $F(\bar{A}) \approx 0$, where $\bar{A}$ is a finite dimensional approximation of the unknowns A with same dimension as F.

The first order data: In the case $\alpha = 0$ or $\alpha = 1$, we have additional unknowns hence we also need to add phase conditions. For the periodic orbit γ, the period τ is an unknown. For the eigenvalue equation defining the stable/unstable bundles it is the eigenvalue/Floquet exponent which is unknown. In both cases we must balance the equations.

For the periodic orbit $\gamma(t)$, we replace $h(v(t),t)$ by the given vector field $g(v(t))$. Note that for any s, the time translated solution $\gamma_s(t) = \gamma(t+s)$ is still a solution of the problem since it is periodic and satisfies $\dot{\gamma_s}(t) = g(\gamma_s(t))$. In order to reject those potential time translation and properly isolate a solution of the problem we set the following Poincaré condition

$$\dot{p_0} \cdot (p_0 - \gamma(0)) = 0, \tag{14}$$

for some $p_0 \in \mathbb{R}^M$ with $\dot{p_0} := g(p_0)$. This condition translates into a condition on $v^1(-1)$ after applying the proper change of variable which is rewritten in term of the Chebyshev coefficients as

$$\dot{p_0} \cdot p_0 - \sum_{j=1}^{M} \dot{v_0}^{(j)} \left(a_{0,0}^{(1,j)} + 2 \sum_{k=1}^{\infty} a_{0,k}^{(1,j)} (-1)^k \right) = 0. \tag{15}$$

So that now we have enough equations to uniquely determine a solution (L, A) that will represent a periodic orbit of $\dot{v}(t) = g(v(t))$.

The normal bundle satisfies the linear equation

$$\dot{v}(t) = Dg(\gamma(t))v(t) - \lambda v(t),$$

where $Dg(\gamma(t))$ is the periodic matrix given by the derivative of g evaluated at the periodic orbit. It follows that any rescaling $kv(t)$ of the bundle will provides a different solution associated to the same eigenvalue λ. To isolate the solution, we fix $\|v(0)\|$ to a given constant K. This condition rewrites in term of the Chebyshev coefficients as

$$\sum_{j=1}^{M} \left(a_0^{(1,j)} + 2 \sum_{k=1}^{\infty} a_k^{(1,j)} (-1)^k \right)^2 - K = 0.$$

For simplicity we truncate this condition to

$$\sum_{j=1}^{M} \sum_{k=0}^{k_0} \left(a_k^{(1,j)} \right)^2 - K = 0, \tag{16}$$

which still isolates an eigenfunction. Thus, the first two cases can now be solved by adding the operator $f^0 : \mathbb{R} \to \mathbb{R}$ to the operator F already given. We define f^0 by the left hand side of (15) for $\alpha = 0$ and the left hand side of (16) for $\alpha = 1$.

4. Examples

We introduce the following operator to simplify the expansion of the operator F in each example.

Definition 4.1. Let $(j_1, \ldots, j_n)$ be a set consisting of hyperscript corresponding to component of the solution. That is $1 \leq j_k \leq M$ for all $k = 1, \ldots, n$, we denote their Cauchy product of convolutions by

$$\mathcal{C}_{\alpha,k}^{(i)}(j_1, \ldots, j_n) = \sum_{\substack{\alpha_1 + \ldots + \alpha_n = \alpha \\ \alpha_j \in \mathbb{Z}^+}} \sum_{\substack{k_1 + \ldots + k_n = k \\ k_j \in \mathbb{Z}}} a_{\alpha_1,k_1}^{(i,j_1)} a_{\alpha_2,k_2}^{(i,j_2)} \cdots a_{\alpha_n,k_n}^{(i,j_n)}.$$

Note that the case $\alpha = 0$ simply returns the convolution product.

4.1. *The example of the Lorenz system*

All of our numerical computations use the classical parameter values $\beta = \frac{8}{3}$, $\rho = 27$ and $\sigma = 10$. The operator defining the unknowns $A_\alpha(t)$ is given by

$$\begin{aligned}
f_{\alpha,k}^{(i,1)}(A_\alpha) &= 2k a_{\alpha,k}^{(i,1)} + L_i \Big(-\lambda \alpha a_{\alpha,k\pm1}^{(i,1)} + \sigma (a_{\alpha,k\pm1}^{(i,2)} - a_{\alpha,k\pm1}^{(i,1)}) \Big) \\
f_{\alpha,k}^{(i,2)}(A_\alpha) &= 2k a_{\alpha,k}^{(i,2)} + L_i \Big(-\lambda \alpha a_{\alpha,k\pm1}^{(i,2)} + \rho a_{\alpha,k\pm1} - \mathcal{C}_{\alpha,k\pm1}^{(i)}(2,3) - a_{\alpha,k\pm1}^{(i,2)} \Big), \\
f_{\alpha,k}^{(i,3)}(A_\alpha) &= 2k a_{\alpha,k}^{(i,3)} + L_i \Big(-\lambda \alpha a_{\alpha,k\pm1}^{(i,3)} + \mathcal{C}_{\alpha,k\pm1}^{(i)}(1,2) - \beta a_{\alpha,k\pm1}^{(i,3)} \Big),
\end{aligned}$$

with $k \geq 1$. The formula for $k = 0$ is omitted since it is already explicitly given in (12). Note that $\mathcal{C}$ involves the lower order terms A_β for $\beta \leq \alpha$ but we are only solving for A_α with the lower order terms fixed.

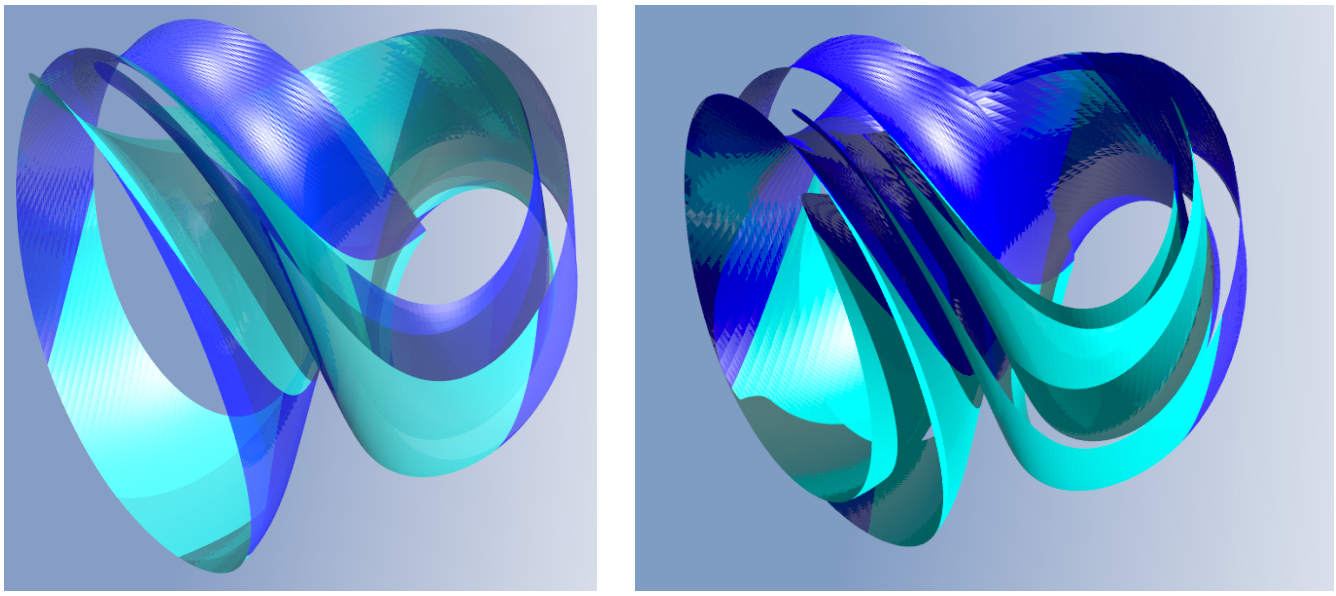

Fig. 5. Periodic orbits ABB (left) and AABBB (right) with their respective stable manifold.

Only the $\alpha = 0$ problem is nonlinear in the unknown Chebyshev coefficients and this requires a good initial guess to obtain a periodic orbit. In the present work we use the data from [Viswanath, 2003] as the input for a Newton method. For each α we truncate and consider the finite dimensional problem

$$\hat{A}_\alpha = \left\{ a_{\alpha,k}^{(i,j)} : 0 \le k \le m-1, 1 \le i \le D, 1 \le j \le 3 \right\}.$$

So that the corresponding truncated operator is such that $F : \mathbb{R}^{3mD+1} \to \mathbb{R}^{3mD+1}$ for $\alpha = 0, 1$ and $F : \mathbb{R}^{3mD} \to \mathbb{R}^{3mD}$ in the remaining cases.

We illustrate the results for some different cases. In Figure 5 we computed the stable manifold for two periodic orbits. For these computations we use $D = 10$ Chebyshev domains, $m = 50$ Chebyshev coefficients per domain, and $N = 50$ Taylor nodes. The integrating time, which is also the value of the time rescale in the operator and half the period, is $L \approx 1.1530$ for the shorter orbit and $L \approx 1.9101$ for the longer one. Each color represent a different subdomain of the Chebyshev time decomposition. The simplicity of the system makes possible to compute many Taylor node for very large values of D without taking too much computing time.

In Figure 6 we extended the manifold on the right of figure 5 by integrating backward in time 100 points evenly distributed on the boundary of the parameterization. The orbits were computed by integrating backward in time for $t = 0.5$. Using the conjugacy relation (4), we have that one would need to integrate for $t = 2.5212$ to go from $\sigma \approx 10^{-16}$ to the boundary $\sigma = 1$. Thus, allowing the utilization of much smaller time lapse to get a good extension of the attractor for this orbit. The discretization of the continued manifold is very coarse, but the example is only included to show that nearly all the "slow" dynamics of the manifold is captured by the parameterization. Once we start integrating the local manifold orbits move away very rapidly.

A-posteriori error analysis: Since computations of local invariant manifolds using the parameterization method are not strictly speaking local, it makes very little sense to speak about the order of the method. This is especially true when we use polynomials of high degree in a large neighborhood of the periodic orbit. Some other notions are needed to quantify the errors in our computations, and as is typical in for the parameterization we exploit the fact that the solution of the invariance equation satisfies a dynamical conjugacy. Numerically checking this conjugacy after the fact leads to a useful notion of defect or a-posteriori error.

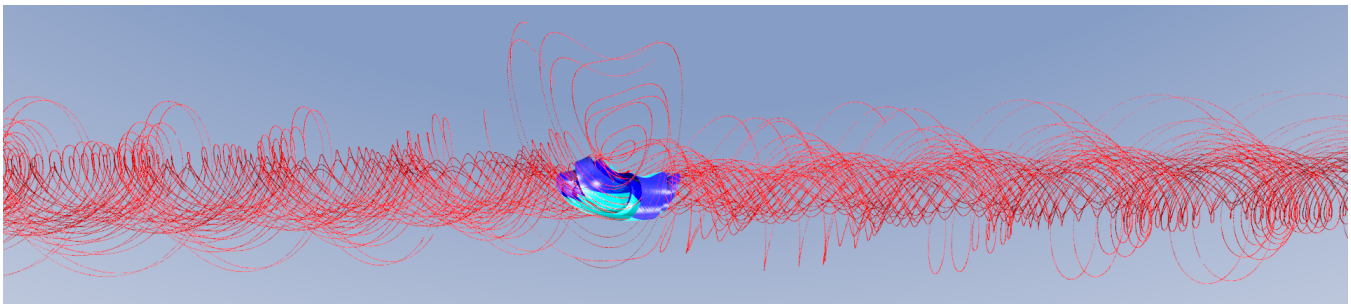

Fig. 6. Periodic orbits AABBB and its stable manifold in blue with orbits in red. The manifold displayed in this figure is the same as in figure 5.

N	$t_0 = 10^{-5}$	$t_0 = 1$
20	9.1859×10^{-4}	4.9280×10^{-1}
40	4.2205×10^{-5}	1.2568×10^{-2}
60	1.2725×10^{-6}	2.6406×10^{-4}
80	3.1854×10^{-8}	8.0463×10^{-6}
100	7.2073×10^{-10}	3.404×10^{-8}

K	$\|a_{100}\|$
50	7.4728×10^{-55}
100	8.4136×10^{-40}
150	5.3647×10^{-31}
200	9.4729×10^{-25}
250	6.6372×10^{-20}

That is, since the equation (4) must be satisfied, we define

$$Err(t_0) := \sup_{s\in[0,\tau]} \sup_{\sigma\in[-1,1]} \left\| P(s+t_0, e^{\lambda t_0}\sigma) - \Phi(P(s,\sigma), t_0) \right\|,$$

and t_0 is some fixed test time. Sampling points in $[0,\tau]$ with $\sigma = \pm 1$ leads to a useful and numerically accessible estimate.

Some heuristics are also helpful. For example we find that choosing N and K so that the norm of the last Taylor component is around machine precision leads to excellent results. A useful norm for making this assessment is

$$\|a_N\| = \max_{i=1,\dots,D} \sum_{j=1}^{3} \sum_{k=0}^{m-1} \left| a_{\alpha,k}^{(i,j)} \right|,$$

as this involves only sums of the known coefficients.

We test the conjugacy for $t_0 = 10^{-5}$ and $t_0 = 1$ with 200 different starting points evenly distributed on the parameterization of the manifold and then took the average of the resulting errors. The results are displayed in table 1. From this table, one can note that the choice of N and K are such that the conjugacy error remains considerably small for longer period of time while the norm of the last Taylor sequence is not too far beyond machine precision.

4.1.1. *Short Connecting orbit*

Following the convention established in [Lessard et al., 2014] we say that we have a short connecting orbit from γ_1 to γ_2 if the local parameterization of the unstable manifold of γ_1 intersects the local parameterization of the stable manifold of γ_2. In this case we establish the existence of a connection with the use of any numerical integration. The fact this this is possible using the parameterization method illustrates again the fact that these computations are in some sense not local.

In Figure 7 we display the stable manifold of the orbit AB and the unstable manifold of ABB in Lorenz and observe several intersection of the two manifolds. The boundary of the unstable manifold crosses the

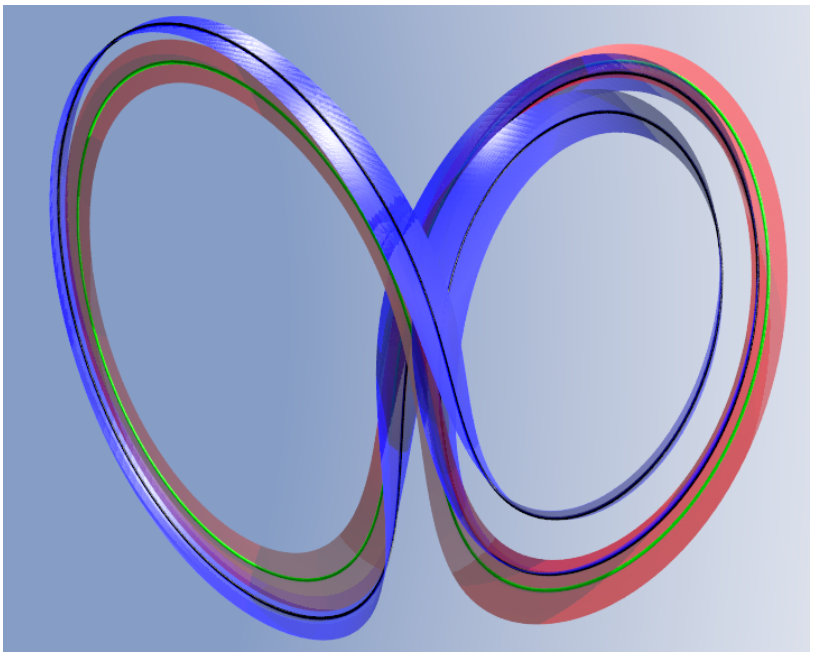

Fig. 7. Unstable manifold of the orbit AB (red) and stable manifold of the ABB orbit (blue). Both manifolds are computed using $m = 100$, $D = 6$, $N = 10$, $K = 10$ and $k_0 = 10$.

stable manifold giving a connecting orbit. Let $P : [0, 2L_1] \times [-1, 1] \to \mathbb{R}^3$ denote the parameterization of the local stable manifold of the periodic orbit AB, whose period is $2L_1$. Similarly, let $Q : [0, 2L_2] \times [-1, 1] \to \mathbb{R}^3$ be the parameterization of the unstable manifold of the periodic orbit ABB, whose period is given by $2L_2$. Once the unstable manifold is restricted to one of its boundary circles only 3 unknowns remain. We set $x = (\theta_s, \sigma_s, \theta_u)$ so that the desired intersection is a zero of

$$S(x) = P(\theta_s, \sigma_s) - Q(\theta_u, 1).$$

Therefore $S : \mathbb{R}^3 \to \mathbb{R}^3$ and it is possible to apply Newton's method to obtain an approximation of the solution. Using this approach, we found

$$x \approx (1.942170529091222, 0.000000560679355, 1.253373698262391).$$

Then the connecting orbit can be computed from those coordinates in the parameter space. Since the value σ_s of x is already quite small we used the conjugacy relation (4) with $t = 2$ and it is already sufficient. For the other half of the connecting orbit, we use (4) again to determine the "time of flight". In this case, the unstable eigenvalue is $\lambda \approx 0.9947$, so one would need to integrate backward in time for $t \approx 34.7246$ to obtain σ smaller than 10^{-15}. Lets stress this point again: computing this orbit using the linear approximation of the stable/unstable manifolds would require almost 35 units of time integration to cross from the unstable to the stable normal bundles. Using the parameterized manifolds no integration is necessary and the entire orbit is represented "locally".

These results are displayed in figure 8. The green curve is the one obtained using the stable manifold while the trajectory in red correspond to the one using the unstable manifold and the time $t = 34.7246$.

4.2. *The Circular Restricted Three Body Problem*

The circular restricted three body problem (CRTBP) studies the movement of a massless particle (or an object with mass considerably smaller than the other two, a satellite for example) moving in the gravitational field of two other massive bodies, called the primaries. It is assumed that the primaries move

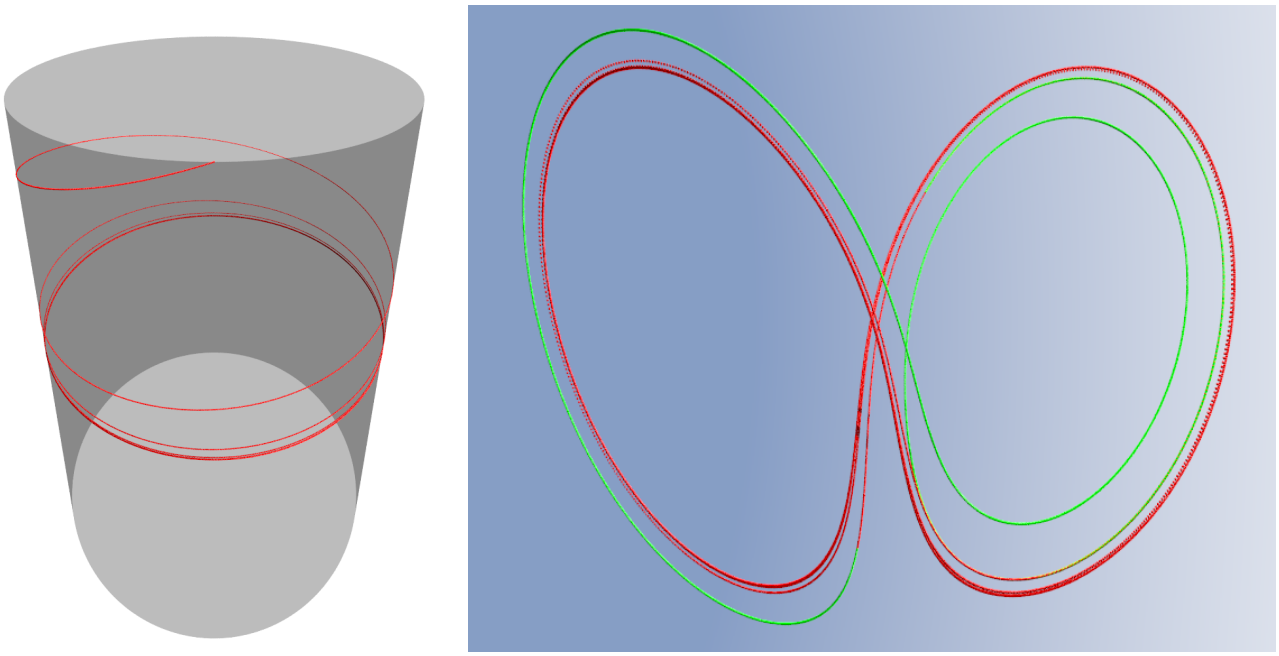

Fig. 8. On the left, trajectory of the orbit in the parameter space of Q, which is periodic in time. On the right, image under P of points for time $t \leq 2$ (green) and image under Q of the trajectory from the left (red).

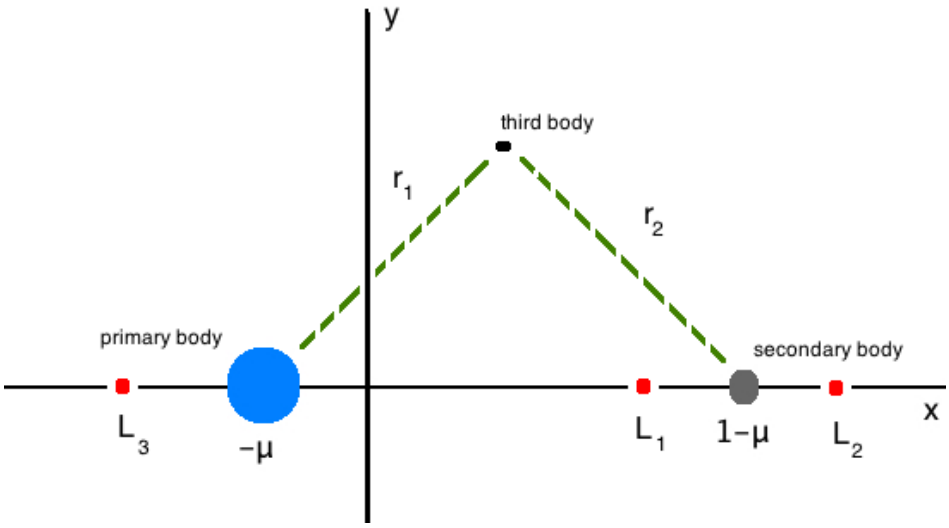

Fig. 9. Schematic representation of the CRTBP: two bodies orbit their common center of mass in a circular orbit. The larger of the two bodies is called the primary and the smaller body is called the secondary. After changing to co-rotating coordinates the primary is located at $x = -\mu, y = 0$ with the smaller body at $x = 1 - \mu, y = 0$. The CRTBP studies the motion of a third and massless particle moving in the gravitational field of the massive particles.

in circular orbits about their center of mass. In co-rotating coordinates the equations of motion are

$$\begin{cases} x'' = 2y' + \frac{\partial H}{\partial x} \\ y'' = -2x' + \frac{\partial H}{\partial y} \end{cases} \tag{17}$$

with

$$H(x,y) = \frac{1}{2}(x^2 + y^2) + \frac{(1-\mu)}{\sqrt{(x+\mu)^2 + y^2}} + \frac{\mu}{\sqrt{(x+\mu-1)^2 + y^2}}.$$

Here μ is the mass ratio of the primary bodies. In the rotating frame:

(1) the center of mass is at the origin,
(2) the motion of the primaries is fixed and they sit on the $x-$axis at $-\mu$ and $1-\mu$.

This choice of coordinates introduces the Coriolis effect. We suppose that the third body moves in the plane of the primaries.

The CRTBP is a much studied system in Hamiltonian dynamics and celestial mechanics as it is a useful model for satellite and astroid motions. It is also one of the simplest N-body systems which admits chaotic motions, hence is not integrable. For more information about the problem or the more general $N-$body problem, we refer the reader to the books of [Belbruno, 2004, 2007; Gómez et al., 2001; Jorba and Masdemont, 1999; Koon et al., 2000; Meyer et al., 2009]. See also [Alessi et al., 2009; Belbruno et al., 2013; Belbruno, 1981; Canalias and Masdemont, 2006; Font et al., 2009; Gómez et al., 2004; Koon et al., 2001; Llibre et al., 1985; Llibre and Simó, 1980; Martí nez and Simó, 2014; Masdemont, 2005]. Again, even this list of references constitutes only the barest introduction to the relevant literature, but much more complete discussion is found in the books and papers just cited.

Rewriting (17) as a vector field $\dot{u} = \hat{g}(u)$ gives

$$\hat{g}(u) = \begin{pmatrix} u^2 \\ 2u^4 + u^1 - \frac{(1-\mu)(u^1+\mu)}{\sqrt{(u^1+\mu)^2+(u^3)^2}^3} - \frac{\mu(u^1-1+\mu)}{\sqrt{(u^1-1+\mu)^2+(u^3)^2}^3} \\ u^4 \\ -2u^2 + u^3 - \frac{(1-\mu)u^3}{\sqrt{(u^1+\mu)^2+(u^3)^2}^3} - \frac{\mu u^3}{\sqrt{(u^1-1+\mu)^2+(u^3)^2}^3} \end{pmatrix} \tag{18}$$

This system is non-polynomial and we propose a related polynomial system through the use of automatic differentiation. Following [Haro, 2016; Lessard et al., 2015] we obtain a system where $M = 6$ and g is a fifth order polynomial given by

$$g(v) = \begin{pmatrix} v^2 \\ 2v^4 + v^1 - (1-\mu)(v^1+\mu)(v^5)^3 - \mu(v^6)^3(v^1-1+\mu) \\ v^4 \\ -2v^2 + v^3 - (1-\mu)v^3(v^5)^3 - \mu v^3(v^6)^3 \\ -(v^5)^3((v^1+\mu)v^2 + v^3v^4) \\ -(v^6)^3((v^1-1+\mu)v^2 + v^3v^4) \end{pmatrix} \tag{19}$$

with the additional (initial condition) constraints

$$v^5(0) = \frac{1}{\sqrt{(v^1(0)+\mu)^2 + (v^3(0))^2}}$$
$$v^6(0) = \frac{1}{\sqrt{(v^1(0)-1+\mu)^2 + (v^3(0))^2}}.$$

Since periodic orbits in the CRTBP occur in one parameter families by varying energy, we fix L and look for a periodic orbit with this half period. Moreover, we use the well known reversible symmetry of the problem to formulate a different boundary condition that will still provide periodic solutions. For example, orbits in a Lyapunov family of one of the co-linear libration points have no velocity in the x direction when they cross the x axis – and the time between the two crossing of the x axis are separated by exactly the half orbit. So that a periodic solution γ starting on the x axis with frequency $2L$ will satisfy

$$\gamma_2(0) = 0, \quad \gamma_3(0) = 0, \quad \gamma_2(2L) = 0 \quad \text{and} \quad \gamma_3(2L) = 0. \tag{20}$$

Remark 4.1. Note that the last two conditions of (20) could also be $\gamma_2(L) = \gamma_3(L) = 0$. This could allow us to compute only the half orbit, the symmetry of the problem providing the solution for the second half of the trajectory. The use of Chebyshev expansion would allow such a choice. However, since the periodic orbit is not the final product of our computations, but only an input into the higher order equations we compute full orbits in this work.

For the remaining two conditions, we simply rewrite the initial condition on v^5 and v^6 after imposing the symmetry, so that

$$\begin{aligned}\gamma^5(0) =& \frac{1}{|\gamma^1(0)+\mu|},\\ \gamma^6(0) =& \frac{1}{|\gamma^1(0)-1+\mu|}.\end{aligned}$$

Due to the choice of the boundary condition, time translation of the solution does not satisfy this system. Thus we drop the Poincaré condition previously given and obtain a system that is still fully determined and with isolated solutions (since we don't solve for the period we dispense with one scalar equation). Two possibilities arise from that remark, one could fix L to a given value and still find an orbit as previously mentioned. The other choice is to use L as a variable and obtain a fully determined system by adding a condition in which the energy level is fixed to a chosen constant. Such a choice is necessary for example if we want to compute heteroclinic connecting orbits.

We summarize the discussion in the following lemma.

Lemma 2. *Let $v^1(t), v^2(t), v^3(t), v^4(t)$ be periodic function with same period ω and such that $\dot{v}^1 = v^2$, $\dot{v}^3 = v^4$. Let $v^5(t), v^6(t)$ be solutions of the boundary value problem*

$$\begin{cases}\dot{v}^5(t) = -(v^5(t))^3((v^1(t)+\mu)v^2(t) + v^3(t)v^4(t)),\\ v^5(0) = \frac{1}{\sqrt{(v^1(0)+\mu)^2+v^3(0)^2}},\end{cases} \tag{21}$$

and

$$\begin{cases}\dot{v}^6(t) = -(v^6(t))^3((v^1(t)-1+\mu)v^2(t) + v^3(t)v^4(t)),\\ v^6(0) = \frac{1}{\sqrt{(v^1(0)-1+\mu)^2+(v^3(0))^2}}.\end{cases} \tag{22}$$

Then $v^5(t)$ and $v^6(t)$ are periodic with period ω.

Proof. We first note that

$$w^5(t) = \frac{1}{\sqrt{(v^1(t)+\mu)^2 + (v^3(t))^2}}$$

is a solution of (21). But by unicity of the solution it follows that $v^5(t) = w^5(t)$. Moreover, we have that $w^5(t)$ is periodic with period ω since $v^1(t)$ and $v^3(t)$ are periodic with period ω. Thus $v^5(t)$ is periodic with period ω, as desired. For $v^6(t)$, the proof is similar using the fact that

$$w^6(t) = \frac{1}{\sqrt{(v^1(t)-1+\mu)^2 + (v^3(t))^2}}$$

is a solution of (22). ■

To fix the energy we have to use an integral of the CRTBP, namely

$$E(x, y, \dot{x}, \dot{y}) = x^2 + y^2 + 2\frac{1-\mu}{\sqrt{(x+\mu)^2+y^2}} + 2\frac{\mu}{\sqrt{(x-1+\mu)^2+y^2}} - (\dot{x}^2 + \dot{y}^2),$$

known as the Jacobi integral. In our system of coordinates, this is

$$E(v^1, v^2, v^3, v^4) := (v^1)^2 + (v^3)^2 + 2(1-\mu)v^5 + 2\mu v^6 - ((v^2)^2 + (v^4)^2).$$

Since E is constant along any orbit of the system, we evaluate it at the endpoint of the first piece of the Chebyshev decomposition. This leads to a new phase condition that can replace the one previously exhibited at equation (15). In terms of the Chebyshev coefficients it is given by

$$f^{(0)}(A_0) = \left(a_{0,0}^{(1,1)} + 2\sum_{k=1}^{\infty} a_{0,k}^{(1,1)}\right)^2 + \left(a_{0,0}^{(1,3)} + 2\sum_{k=1}^{\infty} a_{0,k}^{(1,3)}\right)^2 + 2(1-\mu)\left(a_{0,0}^{(1,5)} + 2\sum_{k=1}^{\infty} a_{0,k}^{(1,5)}\right) + 2\mu\left(a_{0,0}^{(1,6)} + 2\sum_{k=1}^{\infty} a_{0,k}^{(1,6)}\right) - \left(a_{0,0}^{(1,2)} + 2\sum_{k=1}^{\infty} a_{0,k}^{(1,2)}\right)^2 - \left(a_{0,0}^{(1,4)} + 2\sum_{k=1}^{\infty} a_{0,k}^{(1,4)}\right)^2. \tag{23}$$

We now focus on expanding the operator we need to solve in order to obtain the coefficients of the Chebyshev expansion of the $i-$th component of the solution. In the case $k \geq 1$, each case is given by

$$\begin{aligned}
f_{\alpha,k}^{(i,1)}(A_\alpha) &= 2ka_{\alpha,k}^{(i,1)} - L_i\Big(\alpha\lambda a_{\alpha,k\pm1}^{(i,1)} - a_{\alpha,k\pm1}^{(i,2)}\Big),\\
f_{\alpha,k}^{(i,2)}(A_\alpha) &= 2ka_{\alpha,k}^{(i,2)} - L_i\Big(\alpha\lambda a_{\alpha,k\pm1}^{(i,2)} - a_{\alpha,k\pm1}^{(i,1)} - 2a_{\alpha,k\pm1}^{(i,4)} + (1-\mu)\mathcal{C}_{\alpha,k\pm1}^{(i)}(1,5,5,5) + \mu\mathcal{C}_{\alpha,k\pm1}^{(i)}(1,6,6,6)\\
&\qquad + (\mu-\mu^2)\mathcal{C}_{\alpha,k\pm1}^{(i)}(5,5,5) + (\mu^2-\mu)\mathcal{C}_{\alpha,k\pm1}^{(i)}(6,6,6)\Big),\\
f_{\alpha,k}^{(i,3)}(A_\alpha) &= 2ka_{\alpha,k}^{(i,3)} - L_i\Big(\alpha\lambda a_{\alpha,k\pm1}^{(i,3)} - a_{\alpha,k\pm1}^{(i,4)}\Big),\\
f_{\alpha,k}^{(i,4)}(A_\alpha) &= 2ka_{\alpha,k}^{(i,4)} - L_i\Big(\alpha\lambda a_{\alpha,k\pm1}^{(i,4)} + 2a_{\alpha,k\pm1}^{(i,2)} - a_{\alpha,k\pm1}^{(i,3)} + (1-\mu)\mathcal{C}_{\alpha,k\pm1}^{(i)}(3,5,5,5) + \mu\mathcal{C}_{\alpha,k\pm1}^{(i)}(3,6,6,6)\Big),\\
f_{\alpha,k}^{(i,5)}(A_\alpha) &= 2ka_{\alpha,k}^{(i,5)} - L_i\Big(\alpha\lambda a_{1,k\pm1}^{(i,5)} + \mathcal{C}_{\alpha,k\pm1}^{(i)}(1,2,5,5,5) + \mu\mathcal{C}_{\alpha,k\pm1}^{(i)}(2,5,5,5) + \mathcal{C}_{\alpha,k\pm1}^{(i)}(3,4,5,5,5)\Big),\\
f_{\alpha,k}^{(i,6)}(A_\alpha) &= 2ka_{\alpha,k}^{(i,6)} - L_i\Big(\alpha\lambda a_{1,k\pm1}^{(i,6)} + \mathcal{C}_{\alpha,k\pm1}^{(i)}(1,2,6,6,6) + (\mu-1)\mathcal{C}_{\alpha,k\pm1}^{(i)}(2,6,6,6) + \mathcal{C}_{\alpha,k\pm1}^{(i)}(3,4,6,6,6)\Big).
\end{aligned}$$

The cases $k = 0$ are as given in (12) for every $i = 2, \ldots, D$. In the case $i = 1$, we use the condition previously given to rewrite the problem as a zero finding of an operator. Those are given by

$$\begin{aligned}
f_{\alpha,0}^{(1,1)}(A_\alpha) &= a_{0,0}^{(D,2)} + 2\sum_{k=1}^{\infty} a_{0,k}^{(D,2)}(-1)^k,\\
f_{\alpha,0}^{(1,2)}(A_\alpha) &= a_{0,0}^{(D,3)} + 2\sum_{k=1}^{\infty} a_{0,k}^{(D,3)}(-1)^k,\\
f_{\alpha,0}^{(1,3)}(A_\alpha) &= a_{0,0}^{(1,2)} + 2\sum_{k=1}^{\infty} a_{0,k}^{(1,2)},\\
f_{\alpha,0}^{(1,4)}(A_\alpha) &= a_{0,0}^{(1,3)} + 2\sum_{k=1}^{\infty} a_{0,k}^{(1,3)},\\
f_{\alpha,0}^{(1,5)}(A_\alpha) &= \left(a_{0,0}^{(1,5)} + 2\sum_{k=1}^{\infty} a_{0,k}^{(1,5)}(-1)^k\right)\left|a_{0,0}^{(1,1)} + 2\sum_{k=1}^{\infty} a_{0,k}^{(1,1)}(-1)^k + \mu\right| - 1,\\
f_{\alpha,0}^{(1,6)}(A_\alpha) &= \left(a_{0,0}^{(1,6)} + 2\sum_{k=1}^{\infty} a_{0,k}^{(1,5)}(-1)^k\right)\left|a_{0,0}^{(1,1)} + 2\sum_{k=1}^{\infty} a_{0,k}^{(1,1)}(-1)^k - 1 + \mu\right| - 1.
\end{aligned}$$

The operator is now completely determined. In order to approximate the solution we truncate the unknowns and the operator a similar way as for the Lorenz system and obtain an operator such that $F : \mathbb{R}^{6mD+1} \to \mathbb{R}^{6mD+1}$ in the case $\alpha = 0, 1$ and such that $F : \mathbb{R}^{6mD} \to \mathbb{R}^{6mD}$ in the higher dimensional cases. Again, only the search for the periodic orbit requires a good initial guess to obtain the approximation. Following [Lessard et al., 2015] we get an initial guess on which we applied Newton's method. To present results, we regrouped different orbits with the same level of energy.

Fig. 10. Periodic orbits around the Lagragian points $\mathcal{L}_1$ and $\mathcal{L}_2$. The computation displayed were done in the case of the earth-moon ratio $\mu = 0.0123$. Both orbit have energy 3.17

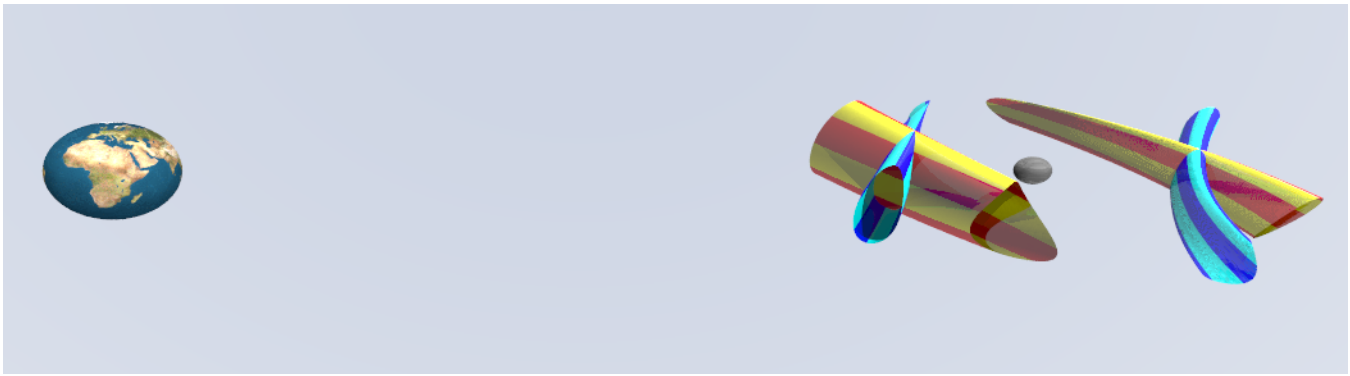

Fig. 11. Stable (blue) and Unstable (red and yellow) manifold for both periodic orbits displayed in figure 10. Manifolds are computed with $N = 10$ Taylor nodes, $m = 50$ Chebyshev coefficients per $D = 8$ Chebyshev domains. The component displayed are v^1, v^2, v^3, that is $x, \dot{x}$ and y in the original system of coordinates.

The figure 10 illustrates two periodic orbits around the equilibrium points $\mathcal{L}_1$ and $\mathcal{L}_2$. Both orbit have energy $E = 3.17$ and have been computed using $m = 50$ Chebyshev nodes and $D = 8$ Chebyshev domains. The integration time L are given by $L \approx 1.7122$ for the orbit around $\mathcal{L}_2$ and $L \approx 1.4242$ for the one around $\mathcal{L}_1$.

In figure 11, one can see the periodic manifolds associated to the two orbits presented in the previous figure. Note that for the sake of simplicity, we fix m to the same value at every step of the same problem. That is, the periodic orbit, the eigenvalue problem and every higher order term of the expansion of the manifold were computed with the same m. However, unlike D, they don't have to be the same values. We also used the same values for different manifold to simplify the code but such a choice is not necessary.

These manifolds were computed using the equation $\dot{v} = g(v(t))$, where g is given by (19). To show that that a point laying in one of those manifolds corresponds to a point on the manifold for the corresponding orbit in the problem without automatic differentiation we use the following Theorem.

Theorem 1. *Let $P(t, \sigma)$ be a parameterization of the local stable manifold of a given periodic orbit $v(t)$ satisfying $\dot{v} = g(v(t))$, where g is given by (19). if $x_0 \in \mathbb{R}^6$ is such that $x_0 = P(t_0, \sigma_0)$, then the point $y_0 \in \mathbb{R}^4$ given by the first four component of x_0 is in the stable set of the corresponding periodic orbit of $\dot{u} = f(u)$, where f is given by (18).*

Proof. Note that using the same remark as in the proof of Lemma (2), we obtain from the periodic orbit $v(t)$ a periodic orbit of the CRTBP. That is a periodic solution of $\dot{u} = f(u(t))$. We denote this orbit by

$u(t)$ and we have that $v^i(t) = u^i(t)$ for $i = 1, 2, 3, 4$, while

$$v^5(t) = \frac{1}{\sqrt{(u^1(t)+\mu)^2 + u^3(t)^2}} \text{ and } v^6(t) = \frac{1}{\sqrt{(u^1(t)-1+\mu)^2 + u^3(t)^2}}.$$

Let $x(t)$ denote the trajectory obtained by flowing x_0 forward in time by $\Phi(v, t)$ the flow solution of $\dot{v} = g(v(t))$. So that, using the conjugacy relation (4), we have

$$x(t) = P(t_0 + t, e^{\lambda t}\sigma_0),$$

where λ is the stable eigenvalue associated to the orbit. Moreover, it follows that

$$\begin{aligned}\dot{x}(t) &= \frac{\partial}{\partial t} P(t_0 + t, e^{\lambda t}\sigma_0) \\ &= \frac{\partial}{\partial t}\Phi(x_0, t) \\ &= g(x(t)).\end{aligned}$$

Thus, by definition of g

$$x^5(t) = \frac{1}{\sqrt{(x^1(t)+\mu)^2 + (x^3(t))^2}} + C_1$$

and

$$x^6(t) = \frac{1}{\sqrt{(x^1(t)-1+\mu)^2 + (x^3(t))^2}} + C_2.$$

Here C_1, C_2 are arbitrary constants. But $x_0 \in W^s(v)$, so that for any $\epsilon > 0$ there exists T such that for all $t \geq T$, we have that

$$\min_{s\in[0,\omega]} \left|x^5(t) - v^5(s)\right| < \epsilon.$$

This force $C_1 = 0$. Similarly, we have that $C_2 = 0$. Now x^5 and x^6 in g are rewritten with the first four component so that g reduce to f and $y(t) = (x^1(t), x^2(t), x^3(t), x^4(t))$ satisfies $\dot{y}(t) = f(y(t))$. Moreover, since $x_0 \in W^s(v)$, we have that $y(t)$ is in the stable set of the corresponding orbit $u(t)$, as desired. ■

4.2.1. *Connecting Orbits*

Again we use the parametrized manifolds to compute connecting orbits between period orbits. In this case we do not find short connections, however using the manifolds a boundary conditions for the connecting orbits substantially reduces the integration time and numerically stabilizes the problem. The behavior of the connecting orbit on the manifold is given by the conjugacy relation.

Remark 4.2. In this work we compute connecting orbits by numerically integrating the system. However, one could adapt the approach developed in section 3 with $\alpha = 0$ to compute any orbit solution of a given boundary value problem expanded as Chebyshev series. This has been done in [Lessard and Reinhardt, 2014; van den Berg et al., 2015; van den Berg and Sheombarsing, 2016] and even leads to computer assisted proofs. We return to this remark in an upcoming work. We also refer to [Arioli, 2002, 2004; Capiński, 2012; Wilczak and Zgliczyński, 2003] for further reading about computer assisted proofs in the CRTBP.

Since the periodic orbits of interest are further from one another than in the Lorenz system, we look for a connecting orbit as the solution of the following problem. Let P and Q denote the parameterization of the stable and unstable manifold and find (θ_u, σ_u), (θ_s, σ_s) within the domain of the corresponding parameterization and the integrating time T such that

$$\Phi(P_0, T) = P(\theta_s, \sigma_s), \tag{24}$$

where $P_0 = Q(\theta_u, \sigma_u)$. The problem stated has five unknowns given by the integrating time and the evaluation of both manifold. Since the trajectories solution of the CRTBP are in $\mathbb{R}^4$, (24) provides four equations and we have one extra variable to the problem. Thus, we fix $\sigma_u = -1$. This choice was made after integrating points from both boundaries and observing which of the two cases was providing orbits going in the direction of the other manifold, therefore providing potential solutions.

Remark 4.3. Recall that the energy is constant along curve solution of the system. Thus, it is impossible to find a connecting orbit between two periodic solution with different energy level. This problem is avoided since the energy is introduced as the phase condition when we solve for the orbit itself. This was done by the definition of $f^{(0)}$ in (23).

Using Newton's method with the unstable manifold of the orbit on the right in figure 10 and the stable manifold of the orbit on the left we found an approximation of a solution to this problem where

$$\begin{aligned}(\theta_u, \sigma_u) &\approx (3.086681925168687, -1)\\ (\theta_s, \sigma_s) &\approx (0.065696587097979, 1)\\ T &\approx 1.654424821513812.\end{aligned}$$

Both manifold were computed with $m = 50$, $D = 8$, $N = 50$, $K = 5$ and $k_0 = 10$. To find an initial guess on which to apply Newton's method we integrated 40 points evenly distributed on the boundary of the unstable manifold and observed that some orbits were potentially intersecting the stable manifold. The connecting orbit and the two manifold are displayed in figure 12.

We also use the conjugacy relation to extend the connecting orbit forward and backward on the manifolds. Integrating in the parameter space until $\sigma_s \approx 10^{-15}$ takes

$$t \approx 12.3688,$$

and for the backward trajectory

$$t \approx 16.1050.$$

The full trajectory is displayed in figure 13. Note that out of the three pieces of the trajectory, only the one in blue was obtained by numerically integrating the system and this piece required the smallest amount of integration time out of them all, approximately 2 units of time. So, using the manifolds the connection requires only 2 units of time rather than about 30.

4.3. *A Circular Restricted Four Body Problem*

In this problem three massive bodies (again called the primaries) are located at the vertices of an equilateral triangle per the equilibrium configuration of Lagrange. These bodies rotate in circular orbits about their common center of mass with the same period so that the triangular shape is rigidly fixed. Now we are interested the motion of a fourth massless particle moving in the resulting gravitational field of the primaries.

We normalize the particle masses m_1, m_2, $m_3 > 0$, so that

$$m_1 + m_2 + m_3 = 1.$$

As in the three body problem it is standard practice to take rotating coordinates which fix the barycenter of the triangle is at the origin and cause the x-axis to bisect the triangle. This places the primaries at positions

$$p_1 = (x_1, y_1, z_1), \qquad p_2 = (x_2, y_2, z_2), \qquad \text{and} \qquad p_3 = (x_3, y_3, z_3),$$

with

$$\begin{aligned}x_1 &= \frac{-|K|\sqrt{m_2^2 + m_2 m_3 + m_3^2}}{K}\\ y_1 &= 0\\ z_1 &= 0\end{aligned}$$

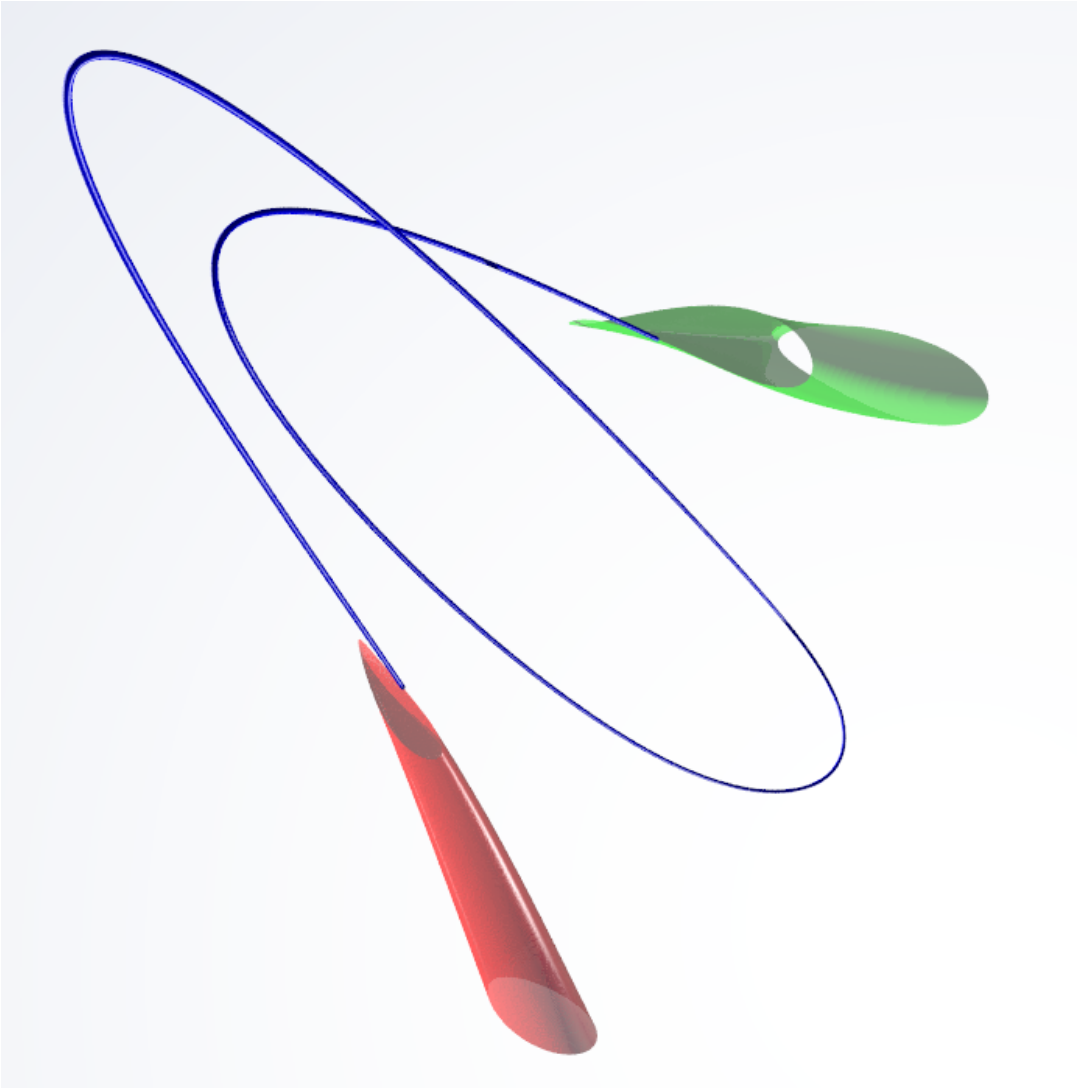

Fig. 12. Connecting orbit between two orbits in the CRTBP using both manifolds to reduce the problem to a finite time. The stable manifold is in green while the unstable is in red.

$$x_2 = \frac{|K|\left[(m_2 - m_3)m_3 + m_1(2m_2 + m_3)\right]}{2K\sqrt{m_2^2 + m_2 m_3 + m_3^2}}$$
$$y_2 = \frac{-\sqrt{3}m_3}{2m_2^{3/2}}\sqrt{\frac{m_2^3}{m_2^2 + m_2 m_3 + m_3^2}}$$
$$z_2 = 0$$

and

$$x_3 = \frac{|K|}{2\sqrt{m_2^2 + m_2 m_3 + m_3^2}}$$
$$y_3 = \frac{\sqrt{3}}{2\sqrt{m_2}}\sqrt{\frac{m_2^3}{m_2^2 + m_2 m_3 + m_3^2}}$$
$$z_3 = 0$$

where

$$K = m_2(m_3 - m_2) + m_1(m_2 + 2m_3).$$

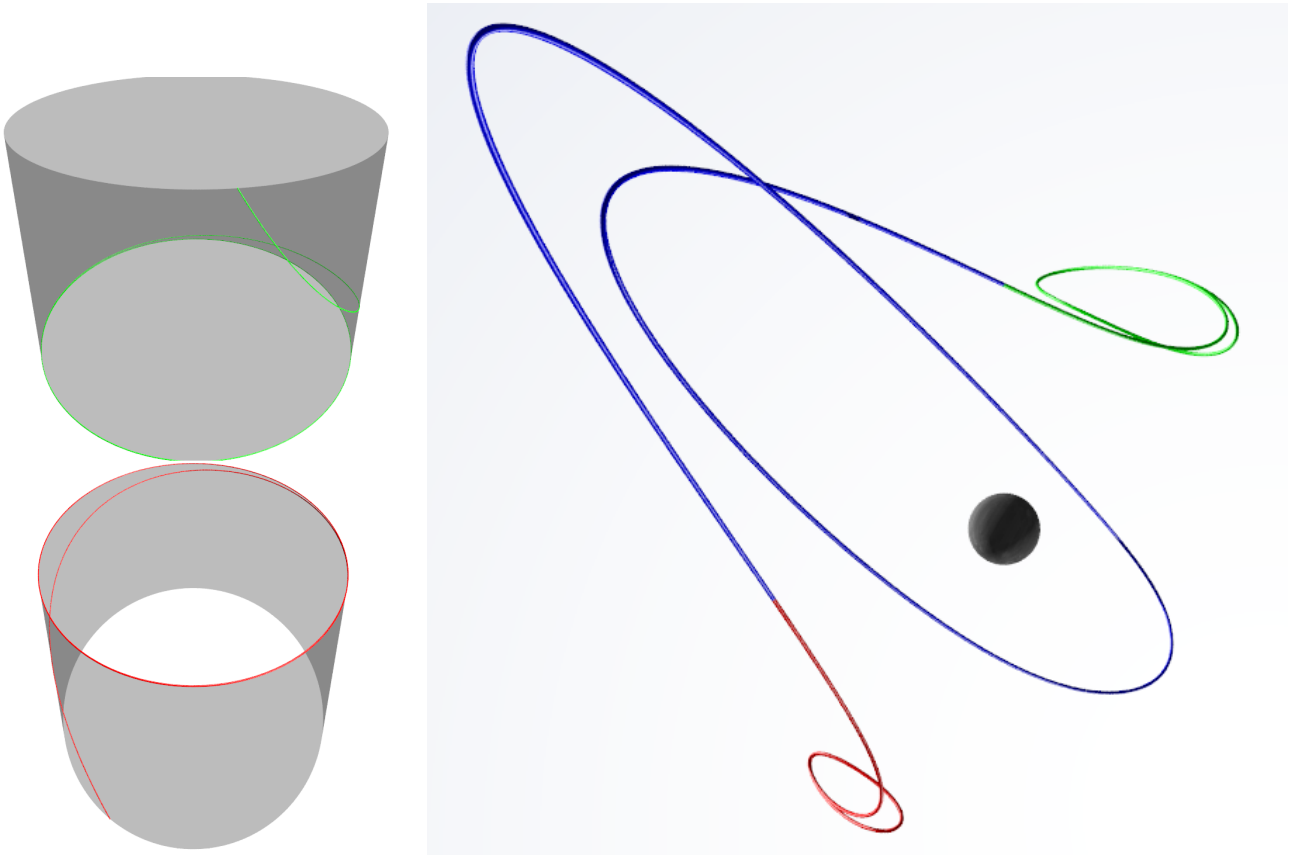

Fig. 13. Extension of the connecting orbit using the parameterization of the manifolds and the conjugacy relation. The trajectories in red and green are integration free/on the manifolds. On the left, the trajectories are displayed in the space of parameters. The top half of the parameter space is displayed for the stable case since σ is positive at all time and the bottom half is displayed for the unstable case.

Define the potential function

$$\Omega(x,y,z) := \frac{1}{2}(x^2+y^2) + \frac{m_1}{r_1(x,y,z)} + \frac{m_2}{r_2(x,y,z)} + \frac{m_3}{r_3(x,y,z)},$$

with

$$r_1(x,y,z) := \sqrt{(x-x_1)^2+(y-y_1)^2+(z-z_1)^2},$$

$$r_2(x,y,z) := \sqrt{(x-x_2)^2+(y-y_2)^2+(z-z_2)^2},$$

and

$$r_3(x,y,z) := \sqrt{(x-x_3)^2+(y-y_3)^2+(z-z_3)^2}.$$

The equations of motion for the massless particle in the co-rotating coordinates are

$$\begin{aligned} \ddot{x} - 2\dot{y} &= \Omega_x, \\ \ddot{y} + 2\dot{x} &= \Omega_y, \\ \ddot{z} &= \Omega_z, \end{aligned} \tag{25}$$

where

$$\frac{\partial}{\partial x}\Omega = \Omega_x(x,y,z) = x - \frac{m_1(x-x_1)}{r_1(x,y,z)^3} - \frac{m_2(x-x_2)}{r_2(x,y,z)^3} - \frac{m_3(x-x_3)}{r_3(x,y,z)^3},$$

$$\frac{\partial}{\partial y}\Omega = \Omega_y(x,y,z) = y - \frac{m_1(y-y_1)}{r_1(x,y,z)^3} - \frac{m_2(y-y_2)}{r_2(x,y,z)^3} - \frac{m_3(y-y_3)}{r_3(x,y,z)^3},$$

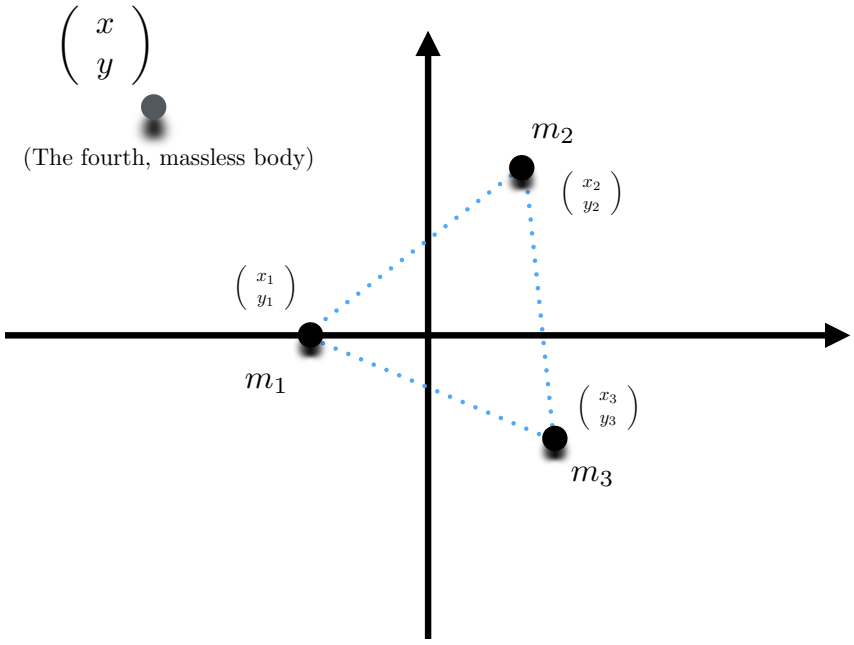

Fig. 14. Schematic representation of the circular restricted four body problem: In this problem three massive primary bodies are arranged in an equilateral triangle configuration. After changing to rotating coordinates which fix the location of the massive bodies, we study a fourth and massless particle moving in the gradational field of the primaries. In this case we allow the fourth body to move out of the plane defined by the triangle.

and

$$\frac{\partial}{\partial z}\Omega = \Omega_z(x,y,z) = -\frac{m_1(z-z_1)}{r_1(x,y,z)^3} - \frac{m_2(z-z_2)}{r_2(x,y,z)^3} - \frac{m_3(z-z_3)}{r_3(x,y,z)^3}.$$

We use automatic differentiation to derive a related polynomial vector field

$$g(v) = \begin{pmatrix} v^2 \\ 2v^4 + v^1 - m_1 v^1 (v^7)^3 - m_2 v^1 (v^8)^3 - m_3 v^1 (v^9)^3 + m_1 x_1 (v^7)^3 + m_2 x_2 (v^8)^3 + m_3 x_3 (v^9)^3 + \beta v^2 \\ v^4 \\ -2v^2 + v^3 - m_1 v^3 (v^7)^3 - m_2 v^3 (v^8)^3 - m_3 v^3 (v^9)^3 + m_1 y_1 (v^7)^3 + m_2 y_2 (v^8)^3 + m_3 y_3 (v^9)^3 \\ v^6 \\ -m_1 v^5 (v^7)^3 - m_2 v^5 (v^8)^3 - m_3 v^5 (v^9)^3 + m_1 z_1 (v^7)^3 + m_2 z_2 (v^8)^3 + m_3 z_3 (v^9)^3 \\ -v^1 v^2 (v^7)^3 - v^3 v^4 (v^7)^3 - v^5 v^6 (v^7)^3 + x_1 v^2 (v^7)^3 + y_1 v^4 (v^7)^3 + z_1 v^6 (v^7)^3 + \alpha_1 (v^7)^3 \\ -v^1 v^2 (v^8)^3 - v^3 v^4 (v^8)^3 - v^5 v^6 (v^8)^3 + x_2 v^2 (v^8)^3 + y_2 v^4 (v^8)^3 + z_2 v^6 (v^8)^3 + \alpha_2 (v^8)^3 \\ -v^1 v^2 (v^9)^3 - v^3 v^4 (v^9)^3 - v^5 v^6 (v^9)^3 + x_3 v^2 (v^9)^3 + y_3 v^4 (v^9)^3 + z_3 v^6 (v^9)^3 + \alpha_3 (v^9)^3 \end{pmatrix}$$

The three bodies having coordinates (x_i, y_i, z_i) for $i = 1, 2, 3$. The constants terms $\beta, \alpha_1, \alpha_2, \alpha_3$ are basically Lagrange multipliers, which are needed to isolate a periodic solution (this time we will not impose any symmetry, hence the boundary condition constraints remain and have to be balanced). The following result, whose proof is found in [Burgos-Garcí a et al., 2017], explains the relation between the polynomial and non-polynomial problems.

Lemma 3. *Assume that $\beta, \alpha_1, \alpha_2, \alpha_3, L \in \mathbb{R}$ are fixed constant with $L > 0$ and let $\boldsymbol{n}, \boldsymbol{p} \in \mathbb{R}^6$ be fixed vector.*

Suppose that $u : [0, 2L] \to \mathbb{R}^9$ *is a periodic solution of* $\dot{v}(t) = g(v)$ *with* g *as above and*

$$\begin{aligned} 0 &= \boldsymbol{n} \cdot ((u^1(0), u^2(0), u^3(0), u^4(0), u^5(0), u^6(0))^T - \boldsymbol{p}) \\ u^7(0) &= \frac{1}{\sqrt{(u^1(0) - x_1)^2 + (u^3(0) - y_1)^2 + (u^5(0) - z_1)^2}} \\ u^8(0) &= \frac{1}{\sqrt{(u^1(0) - x_2)^2 + (u^3(0) - y_2)^2 + (u^5(0) - z_2)^2}} \\ u^9(0) &= \frac{1}{\sqrt{(u^1(0) - x_3)^2 + (u^3(0) - y_3)^2 + (u^5(0) - z_3)^2}} \end{aligned}$$

and that $u^7(t), u^8(t), u^9(t) > 0$ *for all* $t \in [0, 2L]$. *Then*

(1) $\beta = \alpha_1 = \alpha_2 = \alpha_3 = 0$
(2) the function $\hat{u} : [0, 2L] \to \mathbb{R}^6$ *given by*

$$\hat{u}(t) = (u^1(0), u^2(0), u^3(0), u^4(0), u^5(0), u^6(0))^T$$

is a periodic solution of the four body problem.

Yet, the variables $\alpha_1, \alpha_2, \alpha_3$ are not be necessary in the Chebyshev setting since one can use the following lemma to force the initial value condition on v^7, v^8, v^9 without introducing additional equations. The proof is omitted since it is similar to the proof of Lemma 2.

Lemma 4. *Let* $v^1(t), v^2(t), v^3(t), v^4(t), v^5(t), v^6(t)$ *be periodic solution with same period* ω *and such that* $\dot{v}^1 = v^2$, $\dot{v}^3 = v^4$, $\dot{v}^5 = v^6$. *Let* $v^7(t), v^8(t), v^9(t)$ *be solutions of the boundary value problems*

$$\begin{cases} \dot{v}^7(t) = -(v^7(t))^3 \Big((v^1(t) - x_1)v^2(t) + (v^3(t) - y_1)v^4(t) + (v^5(t) - z_1)v^6(t) \Big), \\ v^7(0) = \frac{1}{\sqrt{(v^1(0)-x_1)^2+(v^3(0)-y_1)^2+(v^5(0)-z_1)^2}}, \end{cases}$$

$$\begin{cases} \dot{v}^8(t) = -(v^8(t))^3 \Big((v^1(t) - x_2)v^2(t) + (v^3(t) - y_2)v^4(t) + (v^5(t) - z_2)v^6(t) \Big), \\ v^8(0) = \frac{1}{\sqrt{(v^1(0)-x_2)^2+(v^3(0)-y_2)^2+(v^5(0)-z_2)^2}}, \end{cases}$$

and

$$\begin{cases} \dot{v}^9(t) = -(v^9(t))^3 \Big((v^1(t) - x_3)v^2(t) + (v^3(t) - y_3)v^4(t) + (v^5(t) - z_3)v^6(t) \Big), \\ v^9(0) = \frac{1}{\sqrt{(v^1(0)-x_3)^2+(v^3(0)-y_3)^2+(v^5(0)-z_3)^2}}. \end{cases}$$

Then $v^7(t), v^8(t)$ *and* $v^9(t)$ *are periodic with period* ω.

The extra condition balancing the system is the Poincaré condition which rewrites exactly as in (15). This condition rejects potential time translation of a periodic solution. The other conditions are coming from automatic differentiation and are given by

$$\begin{aligned} v^7(0)^2\big((v^1(0) - x_1)^2 + (v^3(0) - y_1)^2 + (v^5(0) - z_1)^2\big) - 1 = 0, \\ v^8(0)^2\big((v^1(0) - x_2)^2 + (v^3(0) - y_2)^2 + (v^5(0) - z_2)^2\big) - 1 = 0, \\ v^9(0)^2\big((v^1(0) - x_3)^2 + (v^3(0) - y_3)^2 + (v^5(0) - z_3)^2\big) - 1 = 0. \end{aligned}$$

The boundary condition for each Chebyshev subdomain being used for this problem define the operators $f^{(i,j)}_{\alpha,0}$ as previously given in (12) and (13). For all $1 \leq i \leq D$, the case for $k \geq 1$ are given by

$$
\begin{aligned}
f^{(i,1)}_k(A) &= 2ka^{(i,1)}_{\alpha,k} + L_i\Big(-\alpha\lambda a^{(i,1)}_{\alpha,k\pm1} + a^{(i,2)}_{\alpha,k\pm1}\Big),\\
f^{(i,2)}_k(A) &= 2ka^{(i,2)}_{\alpha,k} + L_i\Big(-\alpha\lambda a^{(i,2)}_{\alpha,k\pm1} + 2a^{(i,4)}_{\alpha,k\pm1} + a^{(i,1)}_{\alpha,k\pm1} + \beta a^{(i,2)}_{\alpha,k\pm1}\\
&\qquad - m_1\mathcal{C}^{(i)}_{\alpha,k\pm1}(1,7,7,7) - m_2\mathcal{C}^{(i)}_{\alpha,k\pm1}(1,8,8,8) - m_3\mathcal{C}^{(i)}_{\alpha,k\pm1}(1,9,9,9)\\
&\qquad + m_1x_1\mathcal{C}^{(i)}_{\alpha,k\pm1}(7,7,7) + m_2x_2\mathcal{C}^{(i)}_{\alpha,k\pm1}(8,8,8) + m_3x_3\mathcal{C}^{(i)}_{\alpha,k\pm1}(9,9,9)\Big),\\
f^{(i,3)}_k(A) &= 2ka^{(i,3)}_{\alpha,k} + L_i\Big(-\alpha\lambda a^{(i,3)}_{\alpha,k\pm1} + a^{(i,4)}_{\alpha,k\pm1}\Big),\\
f^{(i,4)}_k(A) &= 2ka^{(i,4)}_{\alpha,k} + L_i\Big(-\alpha\lambda a^{(i,4)}_{\alpha,k\pm1} - 2a^{(i,2)}_{\alpha,k\pm1} + a^{(i,3)}_{\alpha,k\pm1}\\
&\qquad - m_1\mathcal{C}^{(i)}_{\alpha,k\pm1}(3,7,7,7) - m_2\mathcal{C}^{(i)}_{\alpha,k\pm1}(3,8,8,8) - m_3\mathcal{C}^{(i)}_{\alpha,k\pm1}(3,9,9,9)\\
&\qquad + m_1y_1\mathcal{C}^{(i)}_{\alpha,k\pm1}(7,7,7) + m_2y_2\mathcal{C}^{(i)}_{\alpha,k\pm1}(8,8,8) + m_3y_3\mathcal{C}^{(i)}_{\alpha,k\pm1}(9,9,9)\Big),\\
f^{(i,5)}_k(A) &= 2ka^{(i,5)}_{\alpha,k} + L_i\Big(-\alpha\lambda a^{(i,5)}_{\alpha,k\pm1} + a^{(i,6)}_{\alpha,k\pm1}\Big),\\
f^{(i,6)}_k(A) &= 2ka^{(i,6)}_{\alpha,k} + L_i\Big(-\alpha\lambda a^{(i,6)}_{\alpha,k\pm1} - m_1\mathcal{C}^{(i)}_{\alpha,k\pm1}(5,7,7,7) - m_2\mathcal{C}^{(i)}_{\alpha,k\pm1}(5,8,8,8) - m_3\mathcal{C}^{(i)}_{\alpha,k\pm1}(5,9,9,9)\\
&\qquad + m_1z_1\mathcal{C}^{(i)}_{\alpha,k\pm1}(7,7,7) + m_2z_2\mathcal{C}^{(i)}_{\alpha,k\pm1}(8,8,8) + m_3z_3\mathcal{C}^{(i)}_{\alpha,k\pm1}(9,9,9)\Big),\\
f^{(i,7)}_k(A) &= 2ka^{(i,7)}_{\alpha,k} + L_i\Big(-\alpha\lambda a^{(i,7)}_{\alpha,k\pm1} - \mathcal{C}^{(i)}_{\alpha,k\pm1}(1,2,7,7,7) - \mathcal{C}^{(i)}_{\alpha,k\pm1}(3,4,7,7,7) - \mathcal{C}^{(i)}_{\alpha,k\pm1}(5,6,7,7,7)\\
&\qquad + x_1\mathcal{C}^{(i)}_{\alpha,k\pm1}(2,7,7,7) + y_1\mathcal{C}^{(i)}_{\alpha,k\pm1}(4,7,7,7) + z_1\mathcal{C}^{(i)}_{\alpha,k\pm1}(6,7,7,7)\Big),\\
f^{(i,8)}_k(A) &= 2ka^{(i,8)}_{\alpha,k} + L_i\Big(-\alpha\lambda a^{(i,8)}_{\alpha,k\pm1} - \mathcal{C}^{(i)}_{\alpha,k\pm1}(1,2,8,8,8) - \mathcal{C}^{(i)}_{\alpha,k\pm1}(3,4,8,8,8) - \mathcal{C}^{(i)}_{\alpha,k\pm1}(5,6,8,8,8)\\
&\qquad + x_2\mathcal{C}^{(i)}_{\alpha,k\pm1}(2,8,8,8) + y_2\mathcal{C}^{(i)}_{\alpha,k\pm1}(4,8,8,8) + z_2\mathcal{C}^{(i)}_{\alpha,k\pm1}(6,8,8,8)\Big),\\
f^{(i,9)}_k(A) &= 2ka^{(i,9)}_{\alpha,k} + L_i\Big(-\alpha\lambda a^{(i,9)}_{\alpha,k\pm1} - \mathcal{C}^{(i)}_{\alpha,k\pm1}(1,2,9,9,9) - \mathcal{C}^{(i)}_{\alpha,k\pm1}(3,4,9,9,9) - \mathcal{C}^{(i)}_{\alpha,k\pm1}(5,6,9,9,9)\\
&\qquad + x_3\mathcal{C}^{(i)}_{\alpha,k\pm1}(2,9,9,9) + y_3\mathcal{C}^{(i)}_{\alpha,k\pm1}(4,9,9,9) + z_3\mathcal{C}^{(i)}_{\alpha,k\pm1}(6,9,9,9)\Big),
\end{aligned}
$$

Again, we solve recursively the truncated operator to obtain an approximation of the manifold. The case $\alpha = 0$ will have the extra variable β from Lemma (3) and the case $\alpha = 1$ will have the eigenvalue as an extra unknown. Note that in this case we fix the frequency L to a constant, it is still possible to find a solution for the same reason as mentioned in the case of the CRTBP. In figure 15, we display the unstable manifold for a planar orbit of the four body problem. That is $z = 0$ on the periodic orbit. The computation were done with $D = 4$ and $N = 60$. We used masses

$$m_1 \approx 0.9987,\ m_2 \approx 0.0010 \text{ and } m_3 \approx 0.0002.$$

The orbit displayed lays near the heavier mass. In that case a uniform mesh was not suitable since it gets harder to obtain an accurate approximation as the orbit approach one of the bodies. Thus, we took

$$L_1 = 0.0907L,\ L_2 = 0.607L,\ L_3 = .22L \text{ and } L_4 = 0.0823L.$$

However, note that the propositions sum to 1, thus not changing the total integrating time for the problem. To see why the accuracy is affected as the orbit approach a body, recall that the variables arising from automatic differentiation are inversely proportional to the distance between the object and the corresponding

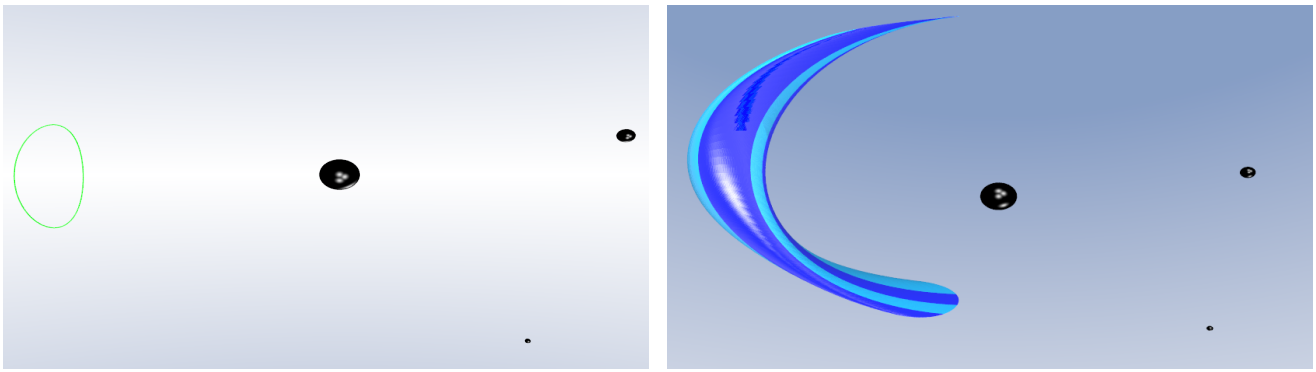

Fig. 15. Planar orbit of the four body problem (left) and its stable manifold (right). The components displayed are (x, y, z) on the left and $(x, \dot{x}, y)$ on the right.

primary, thus provoking a considerable change in the amplitude of the variable.

4.3.1. *Connecting Orbits*

For this problem we focus on an example of a homoclinic connection, hence there are no energy considerations. Heteroclinic connecting orbits are handled as in the three body case. For the periodic orbit displayed in figure 15 we computed both the stable and unstable manifold and apply the same approach as for the CRTBP. In this case the problem still has the same dimension as it has variables since we can get rid of z and $\dot{z}$, which are both 0. Again, the connecting orbits computed start from the boundary of the unstable manifold and ends on the boundary of the stable manifold. The conjugacy relation is used to extend the orbit without integration. In this case both eigenvalues have the same value with opposite signs, so the integrating time forward or backward needed is the same. In order to get from the boundary of the invariant manifold to $\sigma \approx 10^{-15}$ close to the periodic orbit (zero section in parameter space), one needs to integrate for $t = 641.679919$ and we see that the manifolds absorb a quite long approach to the periodic orbit.

Both manifold are computed using $N = 50$, $D = 4$, $m = 50$, $K = 2$ and $k_0 = 10$. We computed a connecting orbit for both piece of the boundary. In the case out of $\sigma_u = 1$, the coordinates for the connecting orbit are

$$\begin{aligned}(\theta_u, \sigma_u) &\approx (0.502504125750113, 1)\\ (\theta_s, \sigma_s) &\approx (5.287357153093578, 1)\\ T &\approx 24.335325092442929.\end{aligned}$$

For the case out of $\sigma_u = -1$, the coordinates are

$$\begin{aligned}(\theta_u, \sigma_u) &\approx (1.6623173901, -1)\\ (\theta_s, \sigma_s) &\approx (4.7735705589, -1)\\ T &\approx 41.3130392127.\end{aligned}$$

The sign of the value σ is affected by the choice of the eigenvector, i.e. the sign determines the polarity of the embedding. In this case we picked the eigenvectors so that the boundaries have the same sign when they lay on the same side of the orbit in the choice of coordinates displayed.

Again, note that the integrating time is smaller than the time needed to integrate on both manifolds. The difference is much bigger since the eigenvalues, given by $\lambda \approx \pm 0.0538$, are closer to zero than in any previous example. The connecting orbit are displayed in figure 16 with both manifolds. The extension of the first orbit using the conjugacy relation is displayed in figure 17. In both cases the coordinates displayed are $(x, y, \dot{y})$.

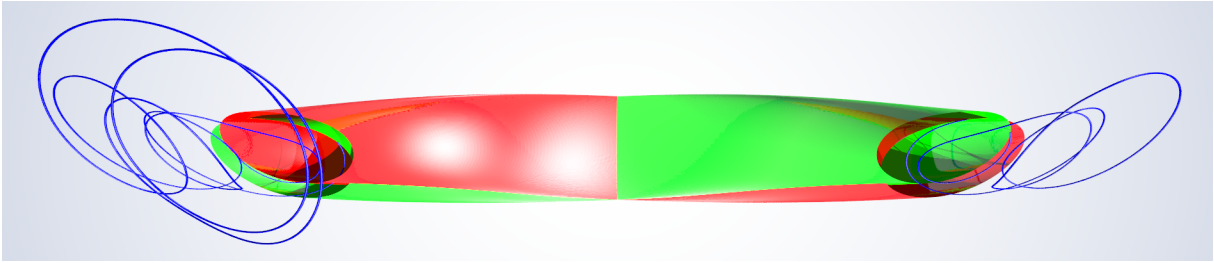

Fig. 16. Homoclinic connections to the orbit displayed in figure 15. The stable manifold is displayed in green while the unstable is in red.

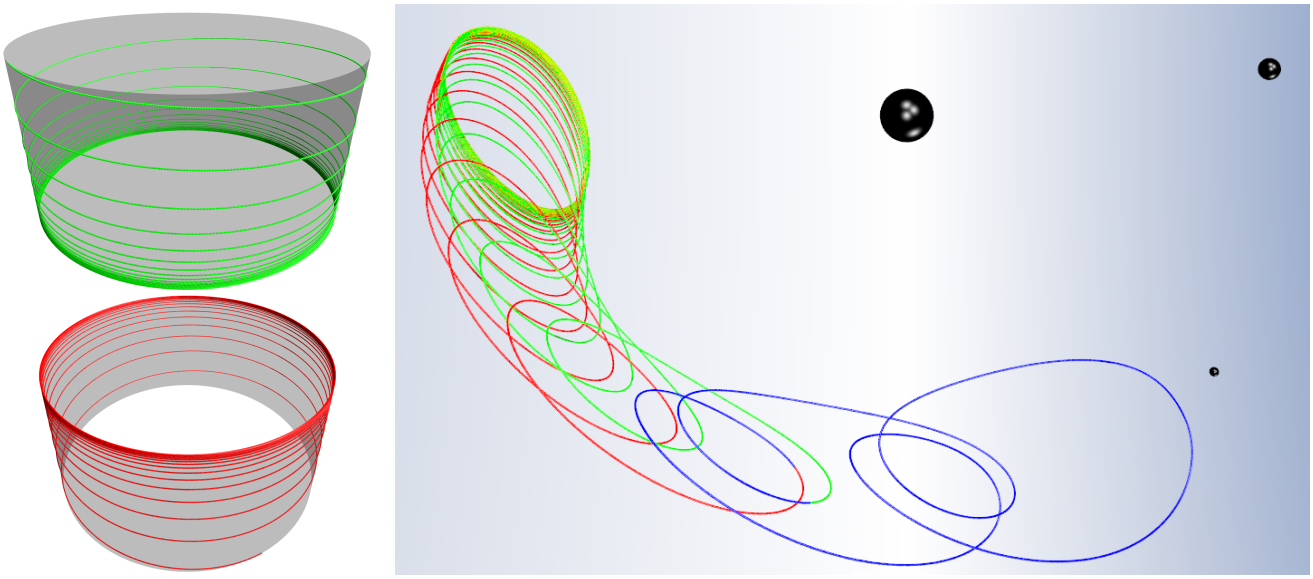

Fig. 17. Extension of the connecting orbit on the right in figure 16 using the parameterization of the manifolds and the conjugacy relation. The trajectories in red and green are integration free. On the left, the trajectories are displayed in the space of parameters. Only the top half of the parameter space is displayed for the stable case since σ is positive at all time.

5. Conclusion

The technique developed allows the computation of periodic manifold. Although every example provided periodic manifold, the technique using Chebyshev expansion does not require the sought after solution to be periodic. This fact was used to introduce domain decomposition in order to improve the accuracy of the parameterization without necessarily increasing the number of Chebyshev coefficients for each expansions. This gave the opportunity to compute relatively large manifold for some high dimensional problems like the four body problem.

In figure 18, we computed the norm of each sequence of Chebyshev expansion in the case of the stable manifold of the orbit AB displayed in figure 4

$$\|a_\alpha^i\| = \sum_{j=1}^{3} \sum_{k=0}^{m-1} \left| a_{\alpha,k}^{(i,j)} \right|,$$

for all $\alpha = 0, \ldots, 100$ and $i = 1, \ldots, 50$. The scale of the eigenvector was chosen so that the norm of the last Taylor dimension is below machine precision in every subdomain. However, one can see from the figure that in this case several component were reaching this magnitude much earlier than some other ones. Such differences arise from the fact that the mesh was uniform in this case. One way to obtain bigger manifold without increasing the chosen dimensions could be to use mesh adaptation, such as in [van den Berg and Sheombarsing, 2016].

By exploiting the properties of Chebyshev expansions of analytic functions, it is possible to construct

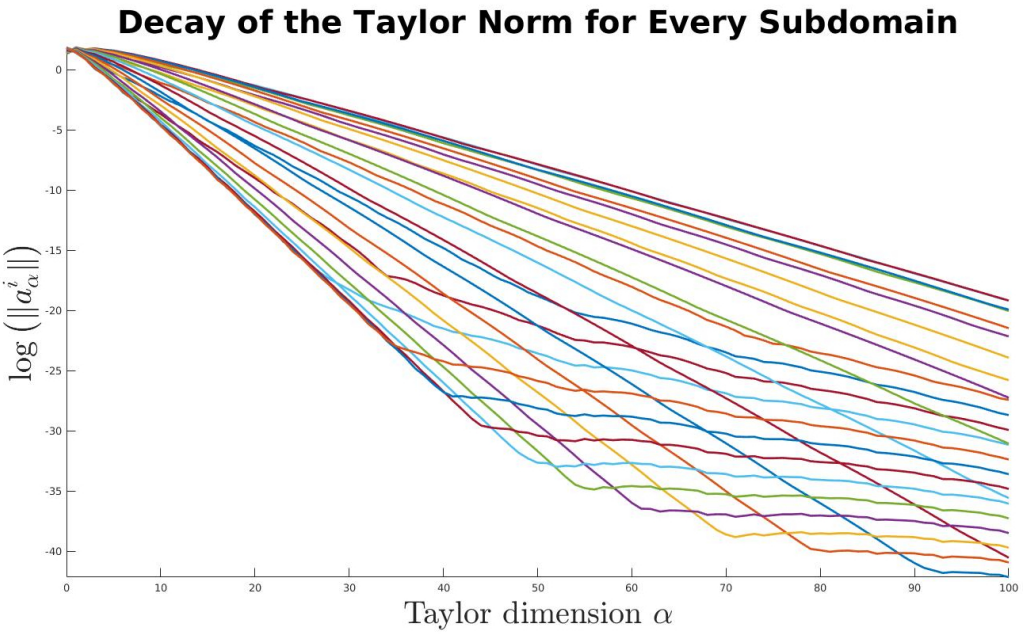

Fig. 18. Decay of the logarithm of the norm of every subdomain. The decay becomes slower once the norm reach machine precision. The "knee" in the decay rates is due to the use of fast Fourier transform to compute convolution products, which tends to stop or slow the decay after machine precision is reached.

an operator defined on the space of coefficients with rapid decay. Then we could use a posteriori analysis and analytic estimates to construct computer assisted arguments that a solution exists using a contraction mapping theorem. This would provide a parameterization of manifold together with rigorous bounds on error estimates. We also remark that there is a possibility that the computations could be sped up by pre-computing the Floquet normal form as in [Castelli et al., 2015]. The Floquet normal form would have to be discretized using Chebyshev rather that Fourier series, and we have not yet explored this possibility.

Acknowledgments

Maxime Murray partially supported by NSF grant DMS-1700154 and by the Alfred P. Sloan Foundation grant G-2016-7320. J.D. Mireles James partially supported by NSF grant DMS-1700154 and by the Alfred P. Sloan Foundation grant G-2016-7320.

References

Alessi, E. M., Gómez, G., and Masdemont, J. J. (2009). Leaving the Moon by means of invariant manifolds of libration point orbits. *Commun. Nonlinear Sci. Numer. Simul.*, 14(12):4153–4167.

Arioli, G. (2002). Periodic orbits, symbolic dynamics and topological entropy for the restricted 3-body problem. *Comm. Math. Phys.*, 231(1):1–24.

Arioli, G. (2004). Branches of periodic orbits for the planar restricted 3-body problem. *Discrete Contin. Dyn. Syst.*, 11(4):745–755.

Belbruno, E. (2004). *Capture dynamics and chaotic motions in celestial mechanics*. Princeton University Press, Princeton, NJ. With applications to the construction of low energy transfers, With a foreword by Jerry Marsden.

Belbruno, E. (2007). *Fly me to the moon*. Princeton University Press, Princeton, NJ. An insider's guide to the new science of space travel, With a foreword by Neil deGrasse Tyson.

Belbruno, E., Gidea, M., and Topputo, F. (2013). Geometry of weak stability boundaries. *Qual. Theory Dyn. Syst.*, 12(1):53–66.

Belbruno, E. A. (1981). A new family of periodic orbits for the restricted problem. *Celestial Mech.*, 25(2):195–217.

Burgos-Garcí a, J., Lessard, J.-P., and Mireles James, J. D. (2017). Halo orbits in the circular restricted four body problem: computer-assisted existence proofs. *(In preperation)*, pages 1–28.

Cabré, X., Fontich, E., and de la Llave, R. (2003a). The parameterization method for invariant manifolds. I. Manifolds associated to non-resonant subspaces. *Indiana Univ. Math. J.*, 52(2):283–328.

Cabré, X., Fontich, E., and de la Llave, R. (2003b). The parameterization method for invariant manifolds. II. Regularity with respect to parameters. *Indiana Univ. Math. J.*, 52(2):329–360.

Cabré, X., Fontich, E., and de la Llave, R. (2005). The parameterization method for invariant manifolds. III. Overview and applications. *J. Differential Equations*, 218(2):444–515.

Canadell, M. and Haro, A. (2014). Parameterization method for computing quasi-periodic reducible normally hyperbolic invariant tori. In *Advances in differential equations and applications*, volume 4 of *SEMA SIMAI Springer Ser.*, pages 85–94. Springer, Cham.

Canalias, E. and Masdemont, J. J. (2006). Homoclinic and heteroclinic transfer trajectories between planar Lyapunov orbits in the sun-earth and earth-moon systems. *Discrete Contin. Dyn. Syst.*, 14(2):261–279.

Capiński, M. J. (2012). Computer assisted existence proofs of Lyapunov orbits at L_2 and transversal intersections of invariant manifolds in the Jupiter-Sun PCR3BP. *SIAM J. Appl. Dyn. Syst.*, 11(4):1723–1753.

Castelli, R., Lessard, J.-P., and Mireles James, J. D. (2015). Parameterization of invariant manifolds for periodic orbits I: Efficient numerics via the Floquet normal form. *SIAM J. Appl. Dyn. Syst.*, 14(1):132–167.

Castelli, R., Lessard, J.-P., and Mireles James, J. D. (2017). Parameterization of invariant manifolds for periodic orbits (ii): a-posteriori analysis and computer assisted error bounds. *(Submitted)*.

Driscoll, T. A., Bornemann, F., and Trefethen, L. N. (2008). The chebop system for automatic solution of differential equations. *BIT*, 48(4):701–723.

England, J. P., Krauskopf, B., and Osinga, H. M. (2005). Computing one-dimensional global manifolds of Poincaré maps by continuation. *SIAM J. Appl. Dyn. Syst.*, 4(4):1008–1041.

Figueras, J.-L. s. and Haro, A. (2012). Reliable computation of robust response tori on the verge of breakdown. *SIAM J. Appl. Dyn. Syst.*, 11(2):597–628.

Figueras, J.-L. s. and Haro, A. (2013). Triple collisions of invariant bundles. *Discrete Contin. Dyn. Syst. Ser. B*, 18(8):2069–2082.

Font, J., Nunes, A., and Simó, C. (2009). A numerical study of the orbits of second species of the planar circular RTBP. *Celestial Mech. Dynam. Astronom.*, 103(2):143–162.

Gameiro, M., Lessard, J.-P., and Ricaud, Y. (2016). Rigorous numerics for piecewise-smooth systems: a functional analytic approach based on Chebyshev series. *J. Comput. Appl. Math.*, 292:654–673.

Gómez, G., Koon, W. S., Lo, M. W., Marsden, J. E., Masdemont, J., and Ross, S. D. (2004). Connecting

orbits and invariant manifolds in the spatial restricted three-body problem. *Nonlinearity*, 17(5):1571–1606.

Gómez, G., Llibre, J., Martí nez, R., and Simó, C. (2001). *Dynamics and mission design near libration points. Vol. I*, volume 2 of *World Scientific Monograph Series in Mathematics*. World Scientific Publishing Co., Inc., River Edge, NJ. Fundamentals: the case of collinear libration points, With a foreword by Walter Flury.

Guillamon, A. and Huguet, G. (2009). A computational and geometric approach to phase resetting curves and surfaces. *SIAM J. Appl. Dyn. Syst.*, 8(3):1005–1042.

Haro, A. (2016). Automatic differentiation methods in computational dynamical systems: Invariant manifolds and normal forms of vector fields at fixed points.

Haro, A., Canadell, M., Figueras, J.-L. s., Luque, A., and Mondelo, J.-M. (2016). *The parameterization method for invariant manifolds*, volume 195 of *Applied Mathematical Sciences*. Springer, [Cham]. From rigorous results to effective computations.

Haro, A. and de la Llave, R. (2006a). A parameterization method for the computation of invariant tori and their whiskers in quasi-periodic maps: numerical algorithms. *Discrete Contin. Dyn. Syst. Ser. B*, 6(6):1261–1300.

Haro, A. and de la Llave, R. (2006b). A parameterization method for the computation of invariant tori and their whiskers in quasi-periodic maps: rigorous results. *J. Differential Equations*, 228(2):530–579.

Haro, A. and de la Llave, R. (2007). A parameterization method for the computation of invariant tori and their whiskers in quasi-periodic maps: explorations and mechanisms for the breakdown of hyperbolicity. *SIAM J. Appl. Dyn. Syst.*, 6(1):142–207.

Huguet, G. and de la Llave, R. (2013). Computation of limit cycles and their isochrons: fast algorithms and their convergence. *SIAM J. Appl. Dyn. Syst.*, 12(4):1763–1802.

Jorba, A. (1999). A methodology for the numerical computation of normal forms, centre manifolds and first integrals of Hamiltonian systems. *Experiment. Math.*, 8(2):155–195.

Jorba, A. and Masdemont, J. (1999). Dynamics in the center manifold of the collinear points of the restricted three body problem. *Phys. D*, 132(1-2):189–213.

Jorba, A. and Villanueva, J. (1998). Numerical computation of normal forms around some periodic orbits of the restricted three-body problem. *Phys. D*, 114(3-4):197–229.

Koon, W. S., Lo, M. W., Marsden, J. E., and Ross, S. D. (2000). Dynamical systems, the three-body problem and space mission design. In *International Conference on Differential Equations, Vol. 1, 2 (Berlin, 1999)*, pages 1167–1181. World Sci. Publ., River Edge, NJ.

Koon, W. S., Lo, M. W., Marsden, J. E., and Ross, S. D. (2001). Low energy transfer to the moon. *Celestial Mech. Dynam. Astronom.*, 81(1-2):63–73. Dynamics of natural and artificial celestial bodies (Poznań, 2000).

Krauskopf, B., Osinga, H. M., Doedel, E. J., Henderson, M. E., Guckenheimer, J., Vladimirsky, A., Dellnitz, M., and Junge, O. (2005). A survey of methods for computing (un)stable manifolds of vector fields. *Internat. J. Bifur. Chaos Appl. Sci. Engrg.*, 15(3):763–791.

Lessard, J.-P., Mireles James, J., and Ransford, J. (2015). Automatic differentiation for fourier series and the radii polynomial approach. *To appear in Physica D*.

Lessard, J.-P., Mireles James, J. D., and Reinhardt, C. (2014). Computer assisted proof of transverse saddle-to-saddle connecting orbits for first order vector fields. *J. Dynam. Differential Equations*, 26(2):267–313.

Lessard, J.-P. and Reinhardt, C. (2014). Rigorous numerics for nonlinear differential equations using chebyshev series. *SIAM Journal on Numerical Analysis*, (52(1)):1–22.

Llibre, J., Martí nez, R., and Simó, C. (1985). Tranversality of the invariant manifolds associated to the Lyapunov family of periodic orbits near L_2 in the restricted three-body problem. *J. Differential Equations*, 58(1):104–156.

Llibre, J. and Simó, C. (1980). Some homoclinic phenomena in the three-body problem. *J. Differential Equations*, 37(3):444–465.

Martí nez, R. and Simó, C. (2014). Invariant manifolds at infinity of the RTBP and the boundaries of bounded motion. *Regul. Chaotic Dyn.*, 19(6):745–765.

Masdemont, J. J. (2005). High-order expansions of invariant manifolds of libration point orbits with applications to mission design. *Dyn. Syst.*, 20(1):59–113.

Masdemont, J. J. (2011). A review of invariant manifold dynamics of the CRTBP and some applications. In *Nonlinear science and complexity*, pages 139–146. Springer, Dordrecht.

Meyer, K., Hall, G., and Offin, D. (2009). *Introduction to Hamiltonian dynamical systems and the N-body problem*, volume 90 of *Applied Mathematical Sciences*. Springer.

Osinga, H. (2000). Non-orientable manifolds of periodic orbits. In *International Conference on Differential Equations, Vol. 1, 2 (Berlin, 1999)*, pages 922–924. World Sci. Publ., River Edge, NJ.

Osinga, H. M. (2003). Nonorientable manifolds in threee-dimensional vector fields. *Internat. J. Bifur. Chaos Appl. Sci. Engrg.*, 13(3):553–570.

Platte, R. B. and Trefethen, L. N. (2010). Chebfun: a new kind of numerical computing. In *Progress in industrial mathematics at ECMI 2008*, volume 15 of *Math. Ind.*, pages 69–87. Springer, Heidelberg.

Simó, C. (1988). Estimates of the error in normal forms of Hamiltonian systems. Applications to effective stability and examples. In *Long-term dynamical behaviour of natural and artificial N-body systems (Cortina d'Ampezzo, 1987)*, volume 246 of *NATO Adv. Sci. Inst. Ser. C Math. Phys. Sci.*, pages 481–503. Kluwer Acad. Publ., Dordrecht.

Simó, C. (1989). On the numerical and analytic approximation of invariant manifolds. In Benest, D. and Froeschlé, C., editors, *Les Methodes Modernes de la Mechanique Céleste*, pages 285–329. Goutelas.

Simó, C. (1998). Effective computations in celestial mechanics and astrodynamics. In *Modern methods of analytical mechanics and their applications (Udine, 1997)*, volume 387 of *CISM Courses and Lect.*, pages 55–102. Springer, Vienna.

Trefethen, L. N. (2007). Computing numerically with functions instead of numbers. *Math. Comput. Sci.*, 1(1):9–19.

Trefethen, L. N. (2013). *Approximation theory and approximation practice*. Society for Industrial and Applied Mathematics (SIAM), Philadelphia, PA.

van den Berg, J. and Sheombarsing, R. (2016). Rigorous numerics for ODEs using Chebyshev series and domain decomposition. Preprint.

van den Berg, J. B., Deschênes, A., Lessard, J.-P., and Mireles James, J. D. (2015). Stationary coexistence of hexagons and rolls via rigorous computations. *SIAM J. Appl. Dyn. Syst.*, 14(2):942–979.

Viswanath, D. (2003). Symbolic dynamics and periodic orbits of the lorenz attractor. *IOP science*, page stacks.iop.org/Non/16/1035.

Wilczak, D. and Zgliczyński, P. (2003). Heteroclinic connections between periodic orbits in planar restricted circular three-body problem - a computer assisted proof. *Comm. Math. Phys.*, 234(1):37–75.